X–ray follow–up work on unassociated sources listed in the *INTEGRAL*/IBIS cat1000 catalogue:

Swift/XRT observations of new objects not present in the 4th *INTEGRAL*/IBIS survey

Raffaella Landi & Loredana Bassani

Report n. 655/2015

June 2015

INAF/IASF Bologna

Introduction

In the following, we provide a report on a number of *Swift*/XRT observations performed so far on unassociated *INTEGRAL*/IBIS sources listed in cat1000 catalogue (Bird et al. 2015, in preparation). More specifically, in this first report we discuss only new source appearing in the catalogue. Results on individual objects are presented and briefly discussed. Simple spectral fitting have been performed on the data to obtain information on the source spectrum only for those sources whose XRT data are of sufficient quality (typically > 50 counts in the source spectrum extraction region) to allow a reliable spectral analysis; quoted column densities are always in excess to the Galactic value in the source direction (Kalberla et al. 2005). In the images reported below, the black circle and the black–dotted circle depict the IBIS 90% and 99% positional uncertainty, respectively. Only X–ray detections above 2.5σ confidence level (c.l.) are reported and discussed.

The *INTEGRAL*/IBIS sources discussed in this report, listed in order of increasing R.A., are the following:

- IGR J00486–4241
- IGR J05288–6840
- IGR J06414–4329
- IGR J07202+0009 (Flag: WARN)
- IGR J07437–5137
- SWIFT J0800.7–4309
- IGR J08030–6853
- SWIFT J0924.2–3141 (Flag: BLEND)
- IGR J12107+0525
- IGR J12207+1517
- IGR J14059–6116
- IGR J14235–1547
- IGR J14319–3315
- IGR J14443–2750
- IGR J15038–6021
- IGR J16181–5407
- IGR J17472+0701
- IGR J18241–1456
- XMMSL1 J182831.3–022901 (PBC J1828.7–0227)
- SWIFT J1839.1+5717

- IGR J20310+3835
- SWIFT J2233.9+1007
- 1SWXRT J230642.8+550817

The multi–wavelength properties of the objects analysed in this work have been collected by exploiting various catalogues and databases reported in the following list:

- United States Naval Observatory B–1.0 catalogue (USNO B–1.0, Monet et al. 2003);
- United States Naval Observatory A–2.0 catalogue (USNO A–2.0, available at: `http://archive.eso.org/skycat/servers/usnoa/`);
- The Two Micron All–Sky Survey (2MASS, Skrutskie et al. 2006);
- Two Micron All Sky Survey Extended Source Survey (2MASX, Skrutskie et al. 2006);
- The Wide–field Infrared Survey Explorer (WISE, Wright et al. 2010);
- The *ROSAT* All–Sky Survey Bright/Faint Source Catalogues (Voges et al. 1999);
- The Galaxy Evolution Explorer All–Sky Survey (GALEX, Bianchi et al. (2011);
- The Second Data Release of the INT Photometric H–Alpha Survey of the Northern Galactic Plane (IPHAS DR2, Barentsen et al. 2014);
- UKIRT Infrared Deep Sky Survey (UKIDSS) Galactic Plane Survey (GPS) (Lucas et al. 2008);
- 6dF Galaxy Survey (6dFGS, Jones et al., 2004;2009)
- CRATES: An All–Sky Survey of Flat-28-Spectrum Radio Sources (Healey et al. 2007);
- The National Radio Astronomy Observatory (NRAO) Very Large Array (VLA) Sky Survey (NVSS, Condon et al. 1998);
- The Magellanic Quasars Survey (MQS, Kozlowski et al. 2013);
- The BeppoSAX Wife Field Cameras (WFC) X–ray source catalogue (Verrecchia et al. 2007);
- The *Swift*/XRT Point Source Catalogue (1SXPS, Evans et al. 2014);
- The *Swift* Serendipitous Survey in deep XRT GRB fields (SwiftFT, Puccetti et al. 2011);
- The *XMM–Newton* Serendipitous Source Catalogue (3XMM–DR4, Watson et al. 2013);
- The *XMM–Newton* Slew Survey Full Source Catalogue (XMMSL1, Saxton et al. 2008);
- The SIMBAD Astronomical Database (available at: `http://simbad.u-strasbg.fr/simbad/`);
- The NASA/IPAC Extragalactic Database (NED, available at: `https://ned.ipac.caltech.edu/`);
- The High Energy Astrophysics Science Archive Research Center provided by NASA's Goddard Space Flight Center (HEASARC, available at: `http://heasarc.gsfc.nasa.gov/`).

IGR J00486–4241

(IBIS detection: persistent)

Two XRT observations available:

1. obscode: 00082524001
   observation date: 01/04/2015
   exposure: 276 s

2. obscode: 00082524002
   observation date: 02/04/2012
   exposure: 1173 s

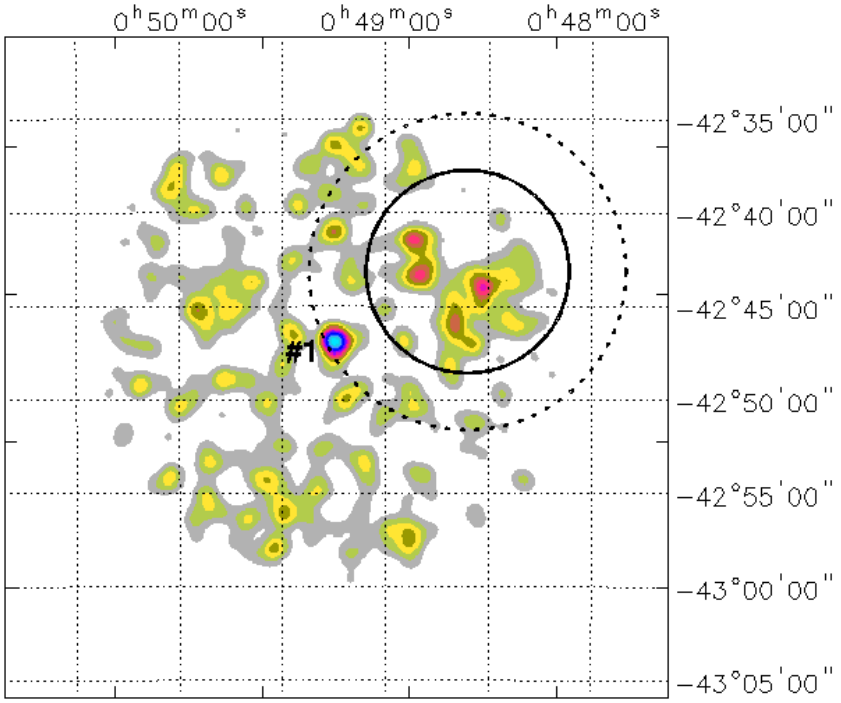

Figure 1: 0.3–10 keV XRT image of the IGR J00486–4241 field.

The only X–ray source detected by XRT is within the 99% IBIS positional uncertainty and is located at:

R.A.(J2000) = $00^{h}49^{m}14'.90$

Dec.(J2000) = $-42^{\circ}46'49''.40$

error box = $6''.00$

It is detected at 2.9σ c.l. in the 0.3–10 keV energy band; no detection is found above 3 keV.

Multi–wavelength counterparts to this XRT detection:

- USNO–A2.0 U0450.00288652 with magnitudes $R = 17.8$, and $B = 18.0$;
- WISE J004914.45–424649.2 with colours $W1 = 14.593 \pm 0.034$, $W2 = 13.394 \pm 0.034$, $W3 = 10.500 \pm 0.065$, and $W4 = 8.485 \pm 0.285$;
- 6dF J0049144–424649; the 6dF spectrum is displayed in Figure 2, but it is of poor quality for a reliable classification;
- *ROSAT* Bright source 1RXS J004913.8–424649 (14 arcseconds error radius);
- J004914.4–424649 listed in the MILLIQUAS catalogue.

Given the poor quality of the XRT data, we can only infer a 2–10 keV flux of $\sim 2 \times 10^{-13}$ erg cm^{-2} s^{-1}, by assuming a power law continuum (photon index frozen to 1.8) passing through the Galactic absorption ($N_{\rm H(Gal)} = 1.47 \times 10^{20}$ cm^{-2}).

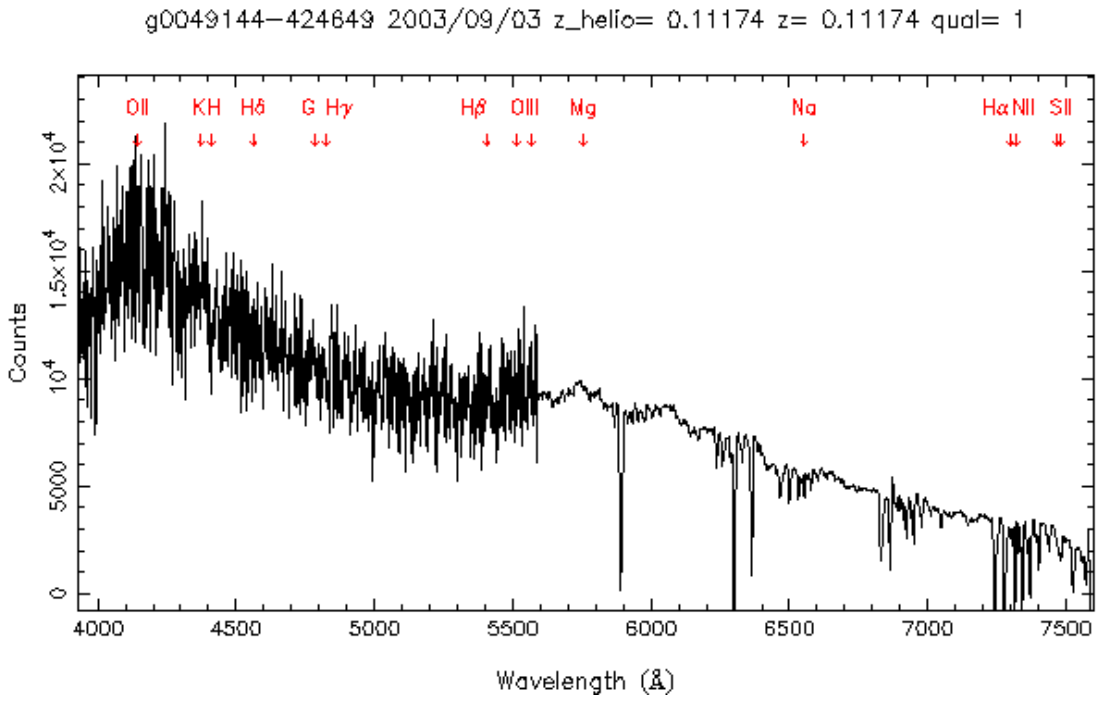

Figure 2: Optical spectrum of 6dF J0049144–424649.

The detection of only one X–ray source in the whole XRT FoV, whose position is compatible with the 99% IBIS positional uncertainty, lead us to propose it as a possible counterpart to the IBIS emitter. Clearly, further X–ray follow–up observations are needed to confirm this suggestion and/or highlight the presence of other soft/X–ray objects not detected so far because of a too low exposure.

IGR J05288–6840

(IBIS detection: 157–day outburst)

Four XRT observations available:

1. obscode: 00045568001
   observation date: 18/03/2012
   exposure: 1467 s
2. obscode: 00045435001
   observation date: 12/11/2012
   exposure: 728 s
3. obscode: 00045435002
   observation date: 16/11/2012
   exposure: 1843 s
4. obscode: 00045568002
   observation date: 28/03/2013
   exposure: 1557 s

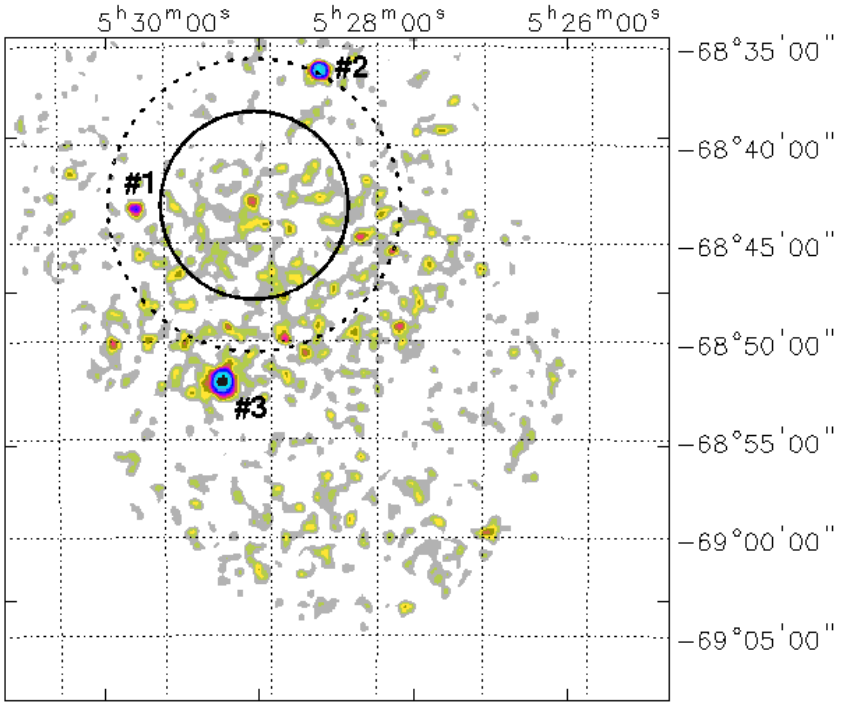

Figure 3: 0.3–10 keV XRT image of the IGR J05288–6840 field.

XRT detects three X–ray objects whose positions are compatible with either the 90% or the 99% IBIS positional uncertainties:

➢ Source #1 is located within the 99% IBIS positional uncertainty at:

R.A.(J2000) = $05^{\rm h}30^{\rm m}15'.10$

Dec.(J2000) = $-68^{\circ}43'13''.90$

error box = $6''.00$

It is detected at 3.3σ and 2.5σ c.l. in the 0.3–10 keV energy band and above 3 keV, respectively.

Multi–wavelength counterparts to this XRT detection:

- USNO–B1.0 0212–0118842 with magnitudes $R2 = 20.84$, and $B2 = 18.72$;
- WISE J053015.24–684315.7 with colours $W1 = 14.541 \pm 0.034$, $W2 = 13.303 \pm 0.029$, $W3 = 10.478 \pm 0.046$, and $W4 = 9.237 \pm 0.354$;
- OGLE LMC 167.7.048443, which belongs to the Magellanic Quasar Survey;
- AGN behind LMC (QSO at $z = 0.616$);
- 3XMM J053015.2–684318 with a 0.2–12 keV flux of $\sim 3.4 \times 10^{-13}$ erg cm^{-2} s^{-1};
- 1SXPS J053016.3–684310.

Given the poor quality of the XRT data, we can only infer a 2–10 keV flux of $\sim 2 \times 10^{-13}$ erg cm^{-2} s^{-1}, by assuming a power law continuum (photon index frozen to 1.8) passing through the Galactic absorption ($N_{\rm H(Gal)} = 2.01 \times 10^{21}$ cm^{-2}).

➢ Source #2 falls at the border of the 99% IBIS error circle and is located at:

R.A.(J2000) = $05^{\rm h}28^{\rm m}32'.70$

Dec.(J2000) = $-68^{\circ}36'12''.00$

error box = $6''.00$

It is detected at 7.3σ c.l. in the 0.3–10 keV energy range, but it is not visible above 3 keV.

Multi–wavelength counterparts to this XRT detection:

- USNO–A2.0 U0150.03129353 with magnitudes $R = 11.1$, and $B = 13.2$;
- 2MASS J05283241–6836135 with magnitudes $J = 9.922 \pm 0.023$, $H = 9.584 \pm 0.027$, and $K = 9.451 \pm 0.021$;
- WISE J052832.40–683613.4 with colours $W1 = 9.301 \pm 0.024$, $W2 = 9.316 \pm 0.020$, $W3 = 9.418 \pm 0.036$, and $W4 = 9.591 \pm 0.000$;
- XMMSL1 J052832.9–683609 ([HP99] 0687) with a 0.2–12 keV flux of $\sim 2.088 \times 10^{-12}$ erg cm^{-2} s^{-1};

- 3XMM J052832.5–683612 with a 0.2–12 keV flux of of $\sim 0.8 \times 10^{-12}$ erg cm^{-2} s^{-1}, which indicates a variable source;
- 1SXPS J052833.1–683611;
- Eclipsing binary of W UMa type HD 269602 of spectral type F8 (variable star).

The X–ray spectrum is modelled with a bremsstrahlung component ($N_{\rm H(Gal)} = 2.06 \times 10^{21}$ cm^{-2}) with $kT \sim 0.5$ keV and a 2–10 keV flux of $\sim 6 \times 10^{-14}$ erg cm^{-2} s^{-1}.

➢ Source #3, which lies outside the 99% IBIS error circle, is located at:

R.A.(J2000) = $05^{\rm h}29^{\rm m}27^{\prime}.38$

Dec.(J2000) = $-68^{\circ}52^{\prime}03^{\prime\prime}.54$

error box = $3^{\prime\prime}.88$

It is detected at 12.8σ c.l. in the 0.3–10 keV energy range, but it is not visible above 3 keV.

Multi–wavelength counterparts to this XRT detection:

- USNO–A2.0 U0150.03149574 with magnitudes $R = 10.1$, and $B = 12.2$;
- 2MASS J05292710–6852048 with magnitudes $J = 8.439 \pm 0.021$, $H = 8.161 \pm 0.047$, and $K = 8.062 \pm 0.023$;
- WISE J052927.13–685204.5 with colours $W1 = 7.990 \pm 0.023$, $W2 = 8.031 \pm 0.020$, $W3 = 8.036 \pm 0.020$, and $W4 = 8.597 \pm 0.179$;
- *ROSAT* Bright source 1RXS J052926.6–685159;
- XMMSL1 J052927.7–685201 with a 0.2–12 keV flux in the range $(1.5 - 2.7) \times 10^{-12}$ erg cm^{-2} s^{-1};
- 3XMM J052926.9-685205 with a 0.2–12 keV flux in the range $(6.4 - 7.0) \times 10^{-13}$ erg cm^{-2} s^{-1}, which indicates some variability;
- 1SXPS J052927.8–685202;
- Eclipsing binary ASAS J052927–6852.0, and rotationally variable star HD 269620 of type G6V.

Because of the poor statistical quality of the data, adopting different spectral model, we find a 2–10 keV flux in the range $5 \times 10^{-14} - 1.1 \times 10^{-12}$ erg cm^{-2} s^{-1}. However, the X–ray spectrum is best modelled with a bremsstrahlung component ($N_{\rm H(Gal)} = 1.96 \times 10^{21}$ cm^{-2}) with $kT \sim 0.6$ keV and a 2–10 keV flux of $\sim 5 \times 10^{-14}$ erg cm^{-2} s^{-1}.

Taking into account the overall properties of the XRT detections, we are led to propose source #1 as a possible counterpart to the IBIS detection, although its spectral properties prevent us from drawing any conclusions about its nature. Moreover, based on the location of source #2 and #3, we discard both objects as possible contributors to the high-energy emission.

IGR J06414–4329

(IBIS detection: 1155.2–day outburst)

Four XRT observations available:

1. obscode: 00035601001
   observation date: 23/06/2006
   exposure: 12343 s
2. obscode: 00035601002
   observation date: 30/06/2006
   exposure: 6696 s
3. obscode: 00047977001
   observation date: 23/08/2013
   exposure: 1005 s
4. obscode: 00080376001
   observation date: 21/01/2014
   exposure: 5198 s

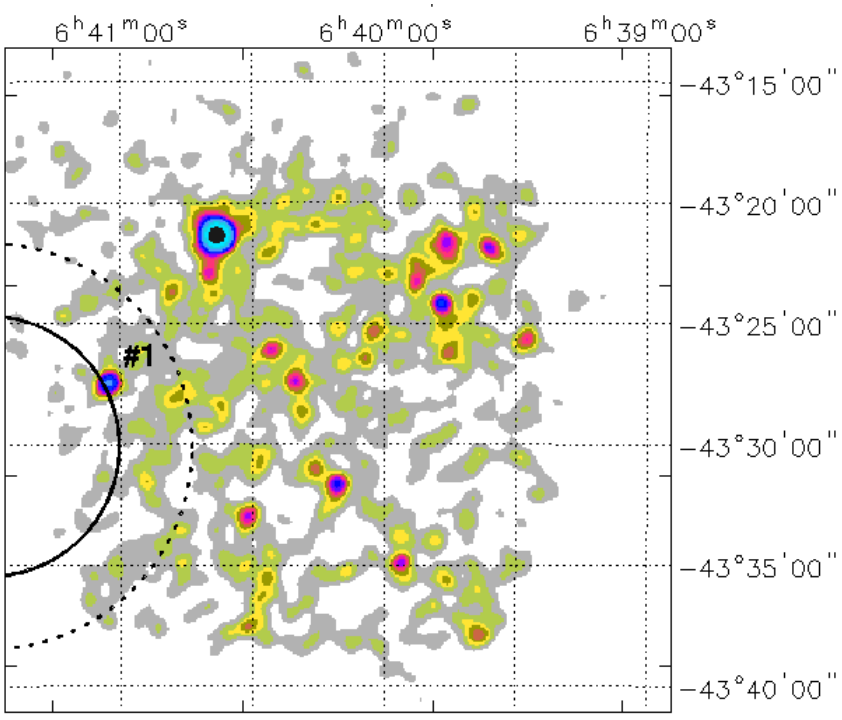

Figure 4: 0.3–10 keV XRT image of the IGR J06414–4329 field. As can be seen from the figure the 90% IBIS error circle partially overlaps the XRT FoV.

As can be seen from Figure 4, both the 90% and 99% IBIS error circles overlap only partially the XRT FoV. In this configuration, the only X–ray detection which is located at the border of the

IBIS positional uncertainty is found at:

R.A.(J2000) = $06^{\rm h}41^{\rm m}02'.50$

Dec.(J2000) = $-43^{\circ}27'26''.60$

error box = $6''.00$

It is detected at 5.3σ c.l. in the 0.3–10 keV energy range, and it is still detected above 3 keV at 2.8σ c.l.

Multi–wavelength counterparts to this XRT detection:

- WISE J064102.62–432727.9 with colours $W1 = 15.261 \pm 0.036$, $W2 = 14.374 \pm 0.042$, $W3 = 11.865 \pm 0.146$, and $W4 = 9.359 \pm 0.000$;
- 1SXPS J064102.7–432728.

The X–ray spectrum of this source, although the poor statistics, is modelled with a simple power law ($N_{\rm H(Gal)} = 5.44 \times 10^{20}$ cm^{-2}) having a photon index around 1.3 and a 2–10 keV flux of $\sim 8 \times 10^{-13}$ erg cm^{-2} s^{-1}.

At this stage, because of the lack of a full coverage of the region surrounding IGR J06414–4329, it is impossible to determine univocally the X–ray counterpart to this high-energy object. The only source detected by XRT is still visible above 3 keV, albeit at only 2.8σ c.l. Further pointed XRT observations are needed to verify the presence/absence of other X–ray sources within the IBIS positional uncertainty.

IGR J07202+0009

(IBIS detection: 1.3–day outburst)

One XRT observation available:

1. obscode: 00067405003
   observation date: 29/05/2005
   exposure: 4751 s

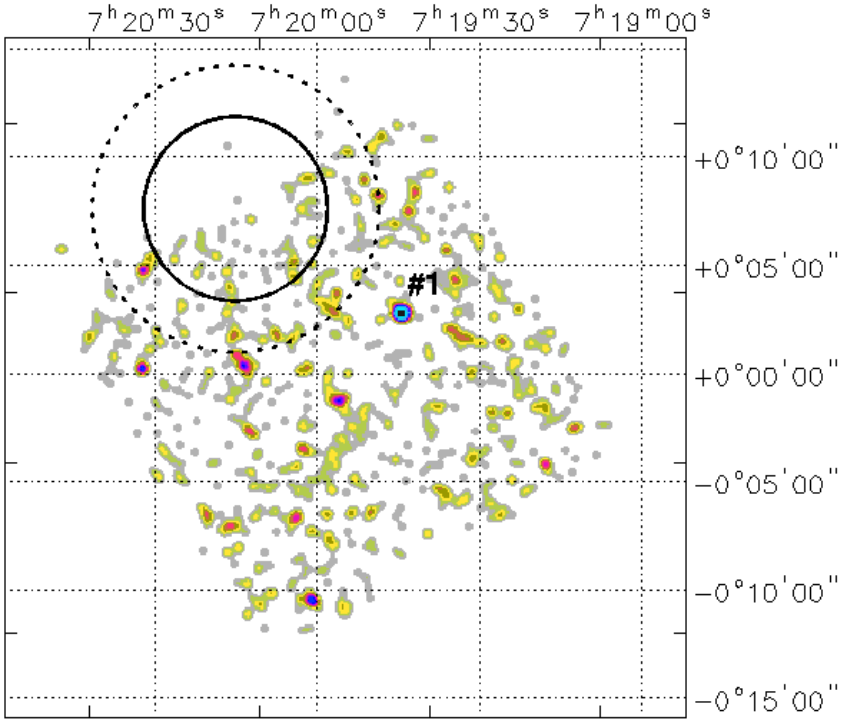

Figure 5: 0.3–10 keV XRT image of the IGR J07202+0009 field.

No X–ray source has been found within both the 90% and the 99% IBIS error circles. The only X–ray source in the XRT field of view, which is detected at 4.8σ c.l. in the 0.3–10 keV energy range but not above 3 keV, is located at:

R.A.(J2000) = $07^{h}19^{m}44^{s}.30$

Dec.(J2000) = $+00°02'48''.40$

error box = $6''.00$

Multi–wavelength counterparts to this XRT detection:

- USNO–A2.0 U0900.04734704 with magnitudes $R = 16.1$, and $B = 16.8$;

- 2MASS J07194439+0002496 with magnitudes $J = 14.998 \pm 0.043$, $H = 14.552 \pm 0.066$, and $K = 14.391 \pm 0.063$;
- WISE J071944.50+000250.0 with colours $W1 = 14.273 \pm 0.037$, $W2 = 13.801 \pm 0.047$, $W3 = 12.061 \pm 0.322$, and $W4 = 8.924 \pm 0.000$.

The location of this object, as well as its lack of detection above 3 keV, leads us to consider unlikely the association with the IBIS emitter. Note also that part of the IBIS error circle is not covered by XRT and that the source is highly variable at high energies.

IGR J07437–5137

(IBIS detection: persistent)

One XRT observation available:

1. obscode: 00037069001
   observation date: 21/09/2007
   exposure: 11920 s

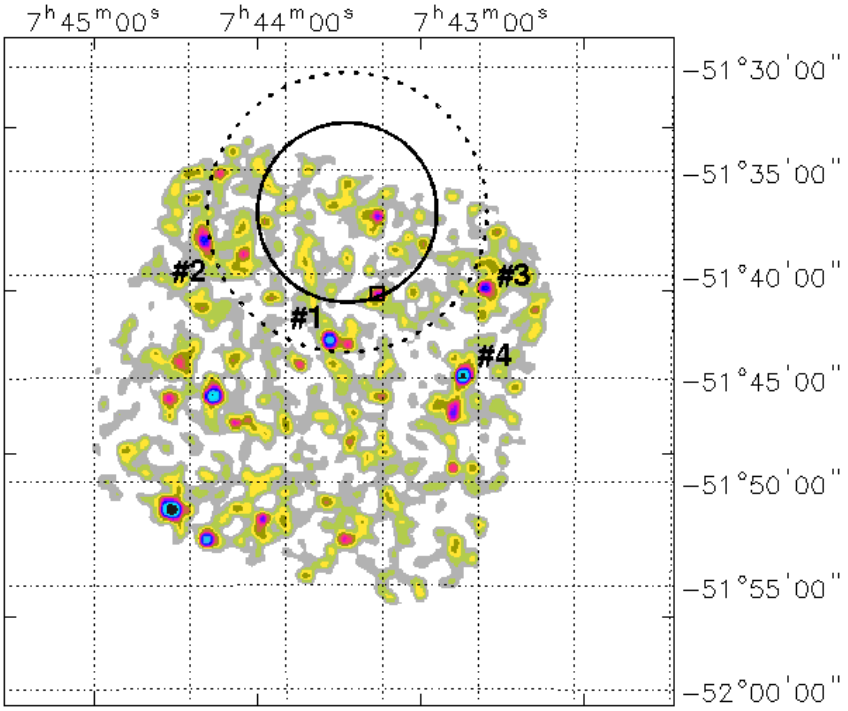

Figure 6: 0.3–10 keV XRT image of the IGR J07437–5137 field. The black box depicts the position of the counterpart to the IBIS object proposed by Masetti et al. (2008), which is not detected in X–rays.

XRT detects three X–ray objects whose positions are compatible with the 99% IBIS positional uncertainty:

➢ Source #1 is located within the 99% IBIS error circle at:

R.A.(J2000) = $07^{h}43^{m}46'.50$

Dec.(J2000) = $-51°43'11''.20$

error box = $6''.00$

It is detected at 3.6σ c.l. in the 0.3–10 keV energy range, and it is not visible above 3 keV.

Multi–wavelength counterparts to this XRT detection:

- USNO–A2.0 U0375.03910519 with magnitudes $R = 11.5$, and $B = 11.6$;
- 2MASS J07434670–5143109 with magnitudes $J = 10.957 \pm 0.024$, $H = 10.713 \pm 0.024$, and $K = 10.604 \pm 0.019$;
- WISE J074346.69–514310.9 with colours $W1 = 10.549 \pm 0.022$, $W2 = 10.713 \pm 0.020$, $W3 = 10.357 \pm 0.043$, and $W4 = 9.411 \pm 0.429$;
- 3XMM J074346.6–514310 with a 0.2–12 keV flux of $\sim 5 \times 10^{-14}$ erg cm^{-2} s^{-1};
- 1SXPS J074346.5–514309;
- Star TYC 8146–873–1.

➢ Source #2 falls at the border of the 99% IBIS error circle and is located at:

R.A.(J2000) = $07^{\rm h}44^{\rm m}25'.10$

Dec.(J2000) = $-51^{\circ}38'20''.40$

error box = $6''.00$

It is detected at 2.8σ c.l. in the 0.3–10 keV energy range, but it is not visible above 3 keV.

Multi–wavelength counterparts to this XRT detection:

- USNO–A2.0 U0375.03929729 with magnitudes $R = 11.0$, and $B = 11.7$;
- 2MASS J07442544–5138193 with magnitudes $J = 10.192 \pm 0.026$, $H = 9.909 \pm 0.023$, and $K = 9.836 \pm 0.023$;
- WISE J074425.44–513819.4 with colours $W1 = 9.769 \pm 0.023$, $W2 = 9.775 \pm 0.021$, $W3 = 9.671 \pm 0.028$, and $W4 = 8.631 \pm 0.201$;
- 3XMM J074425.3–513819 with a 0.2–12 keV flux in the range $(0.038 - 1.4) \times 10^{-12}$ erg cm^{-2} s^{-1}, which indicate strong X–ray variability;
- 1SXPS J074425.1–513819;
- Star TYC 8146–1152–1.

➢ Source #3, which lies just outside the 99% IBIS error circle, is located at:

R.A.(J2000) = $07^{\rm h}42^{\rm m}57'.90$

Dec.(J2000) = $-51^{\circ}40'37''.70$

error box = $6''.00$

It is detected at 3.2σ c.l. in the 0.3–10 keV energy range, but it is not visible above 3 keV.

Multi–wavelength counterparts to this XRT detection:

- USNO–B1.0 0383–0098856 with magnitudes $R2 = 19.68$, and $B2 = 20.74$;
- WISE J074258.58–514038.8 with colours $W1 = 15.510 \pm 0.045$, $W2 = 14.225 \pm 0.041$, $W3 = 11.384 \pm 0.090$, and $W4 = 9.268 \pm 0.362$;
- J074258.6–514039 listed in the MILLIQUAS catalogue;
- 3XMM J074258.6–514038 with a 0.2–12 keV flux of $\sim 4.8 \times 10^{-14}$ erg cm^{-2} s^{-1};
- 1SXPS J074258.2–514039.

There is another X–ray source, which is placed at $\sim$3 arcminutes form the border of the 99% IBIS positional uncertainty, located at:

R.A.(J2000) = $07^{\rm h}43^{\rm m}04'.70$

Dec.(J2000) = $-51^{\circ}44'52''.60$

error box = $6''.00$

It is detected at 4.4σ c.l. in the 0.3–10 keV energy band, and it is still detected above 3 keV at 4.3σ c.l.

Multi–wavelength counterparts to this XRT detection:

- USNO–A2.0 U0375.03890121 ($R = 16.8$, and $B = 18.0$), and USNO–A2.0 U0375.03890399 ($R = 17.2$, and $B = 19.7$);
- 2MASS J07430463–5144557 with magnitudes $J = 16.879 \pm 0.167$, $H = 15.394 \pm 0.000$, and $K = 14.729 \pm 0.000$;
- WISE J074304.55–514455.9 ($W1 = 14.819 \pm 0.037$, $W2 = 14.523 \pm 0.052$, $W3 = 11.000 \pm 0.069$, and $W4 = 8.968 \pm 0.000$), and WISE J074305.26-514455.4 ($W1 = 14.464 \pm 0.032$, $W2 = 14.086 \pm 0.040$, $W3 = 11.366 \pm 0.093$, and $W4 = 8.648 \pm 0.260$);
- 3XMM J074305.3–514455 with a 0.2–12 kev flux of $\sim 2.5 \times 10^{-13}$ erg cm^{-2} s^{-1};
- 1SXPS J074305.0–514454.

IGR J07437–5137 was classified as a Seyfert 2 at $z = 0.025$ by Masetti et al. (2008). Despite the lack of an X–ray counterpart, Masetti and co–workers found a single optical object within the IBIS error circle, whose position is compatible with both a NVSS radio source and a far–IR IRAS one (black box in Figure 6). As can be seen from the Figure, the XRT data confirms the lack of any detection in X–rays from this or any other source inside the IBIS error circle, casting doubts on the real association of the proposed counterpart with the high–energy detection.

SWIFT J0800.7–4309

(IBIS detection: persistent)

Four XRT observations available:

1. obscode: 00041761001
   observation date: 08/12/2010
   exposure: 713 s

2. obscode: 00041761002
   observation date: 12/12/2010
   exposure: 5510 s

3. obscode: 00041761003
   observation date: 15/12/2010
   exposure: 5737 s

4. obscode: 00041761004
   observation date: 16/12/2010
   exposure: 1085 s

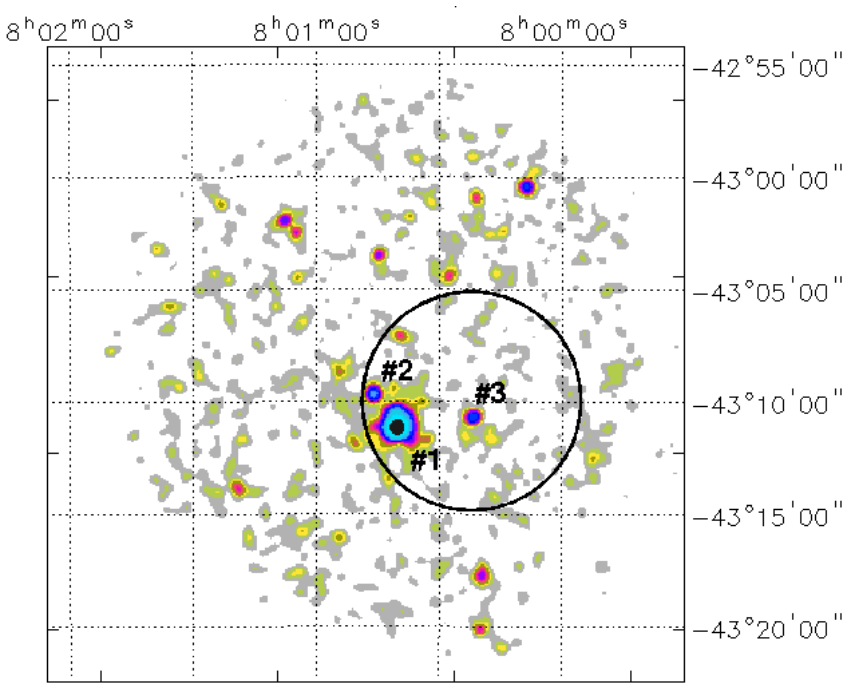

Figure 7: 0.3–10 keV XRT image of the SWIFT J0800.7–4309 field.

There are three X–ray sources within the 90% IBIS positional uncertainty:

➢ Source #1 is located at:

R.A.(J2000) = $08^{\rm h}00^{\rm m}40'.18$

Dec.(J2000) = $-43^{\circ}11'07''.27$

error box = $3''.62$

It is detected at 27.5σ c.l. in the 0.3–10 keV energy band, and it is still observed above 3 keV at 18.3σ c.l.

Multi–wavelength counterparts to this XRT detection:

- USNO–A2.0 U0450.05566363 with magnitudes $R = 16.8$, and $B = 16.5$;
- 2MASS J08003998–4311076 with magnitudes $J = 15.983 \pm 0.103$, $H = 15.732 \pm 0.148$, and $K = 15.575 \pm 0.213$;
- WISE J080039.97–431107.2 with colours $W1 = 15.267 \pm 0.043$, $W2 = 15.124 \pm 0.100$, $W3 = 13.065 \pm 0.000$, and $W4 = 8.818 \pm 0.000$;
- 1SXPS J080039.9–431106.

A simple power law passing through Galactic absorption ($N_{\rm H(Gal)} = 3.53 \times 10^{21}$ cm^{-2}) does not yield a good fit to the data ($\chi^2/\nu = 43.6/36$). The photon index turns out to be flat ($\Gamma = 0.82 \pm 0.11$) and the 2–10 keV flux is around 5×10^{-12} erg cm^{-2} s^{-1}. The residuals to the data shows an excess below 1 keV that we try to model by adopting a double power law model, with the primary component absorbed by intrinsic absorption and the secondary component, having the same photon index of the primary one, passing only through the Galactic column density. The fit, slightly improved ($\Delta\chi^2 = 6.8/3$), provides an intrinsic column density $N_{\rm H(intr)} = \left(6.08^{+3.81}_{-2.59}\right) \times 10^{22}$ cm^{-2}, a photon index $\Gamma = \left(1.55^{+0.43}_{-0.46}\right)$ and a 2–10 keV flux of $\sim 4.7 \times 10^{-12}$ erg cm^{-2} s^{-1}. Unfortunately, there is still the presence of an excess above 0.5 keV.

➢ Source #2 is located at:

R.A.(J2000) = $08^{\rm h}00^{\rm m}45'.80$

Dec.(J2000) = $-43^{\circ}09'37''.90$

error box = $6''.00$

It is detected at 5.7σ and 3.3σ c.l. in 0.3–10 keV energy band and above 3 keV, respectively.

Multi–wavelength counterparts to this XRT detection:

- USNO–A2.0 U0450.05571649 with magnitudes $R = 17.4$, and $B = 17.6$;

- WISE J080045.84–430939.5 with colours $W1 = 15.154 \pm 0.039$, $W2 = 14.651 \pm 0.067$, $W3 = 11.976 \pm 0.217$, and $W4 = 9.426 \pm 0.527$;
- 1SXPS J080045.8–430937.

For this object a simple power law passing through Galactic absorption ($N_{\rm H(Gal)} = 3.55 \times 10^{21}$ cm^{-2}) provides a good fit to the data, yielding a photon index $\Gamma = \left(1.29^{+0.87}_{-0.83}\right)$ and a 2–10 keV flux of $\sim$1.6 $\times$ 10^{-13} erg cm^{-2} s^{-1}.

➢ Source #3 is located at:

R.A.(J2000) = $08^{\rm h}00^{\rm m}21'.40$

Dec.(J2000) = $-43^{\circ}10'40''.80$

error box = $6''.00$

It is detected at 5σ c.l. in the 0.3–10 keV energy band, and it is not observed above 3 keV.

Multi–wavelength counterparts to this XRT detection:

- USNO–A2.0 U0450.05548499 ($R = 15.3$, and $B = 16.8$), USNO–A2.0 U0450.05548418 ($R = 17.3$, and $B = 19.3$), and USNO–A2.0 U0450.05548213 ($R = 17.6$, and $B = 20.2$);
- 2MASS J08002130–4310387 ($J = 16.487 \pm 0.213$, $H = 13.678 \pm 0.000$, and $K = 13.513 \pm 0.000$), and 2MASS J08002130–4310441 ($J = 12.295 \pm 0.023$, $H = 11.593 \pm 0.021$, and $K = 11.368 \pm 0.021$);
- WISE J080021.30–431044.0 with colours $W1 = 11.241 \pm 0.023$, $W2 = 11.150 \pm 0.021$, $W3 = 11.111 \pm 0.095$, and $W4 = 9.339 \pm 0.000$;
- 1SXPS J080021.3–431039.

On the basis of the properties acquired for the XRT detections, we propose source #1 as the putative counterpart to the high-energy emission.

IGR J08030–6853

(IBIS detection: 4.9–day outburst)

One XRT observation available:

1. obscode: 000338177000
   observation date: 26/12/2008
   exposure: 4286 s

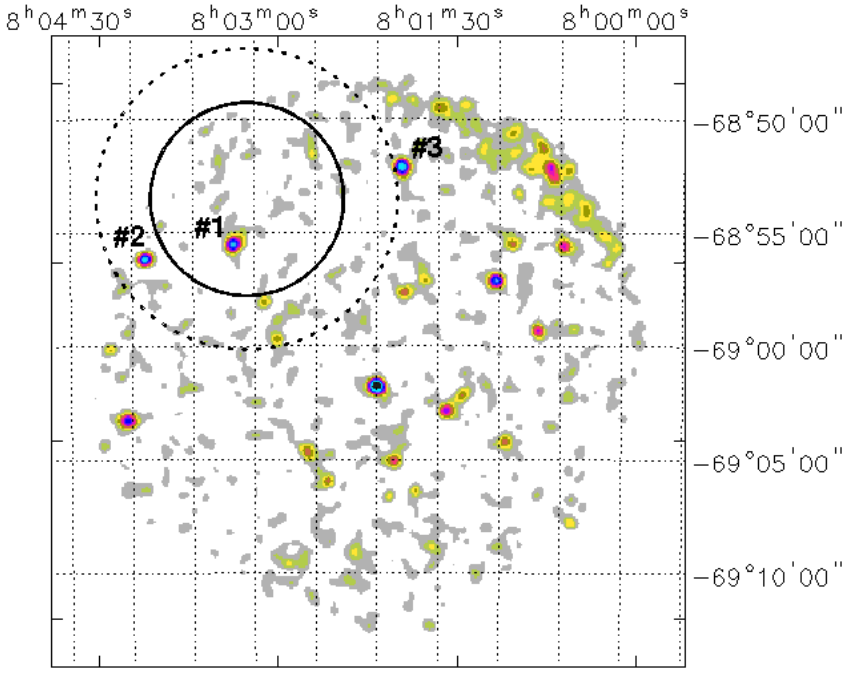

Figure 8: 0.3–10 keV XRT image of the IGR J08030–6853 field.

XRT detects three X–ray objects whose positions are compatible with either the 90% or the 99% IBIS positional uncertainties:

➢ Source #1, which lies inside the 90% IBIS error circle, is located at:

R.A.(J2000) = $08^{h}03^{m}10'.10$

Dec.(J2000) = $-68°55'31''.30$

error box = $6''.00$

It is detected at 4.7σ c.l. in the 0.3–10 keV energy band, but not above 3 keV.

Multi–wavelength counterparts to this XRT detection:

- USNO–A2.0 U0150.05115064 with magnitudes $R = 16.1$, and $B = 17.5$;
- 2MASS J08030985–6855300 ($J = 15.792 \pm 0.101$, $H = 15.243 \pm 0.129$, and $K = 14.867 \pm 0.136$), and 2MASS J08030950–6855270 ($J = 16.085 \pm 0.103$, $H = 15.746 \pm 0.155$, and $K = 15.488 \pm 0.247$);
- WISE J080309.68–685528.5 ($W1 = 14.479 \pm 0.041$, $W2 = 14.564 \pm 0.048$, $W3 = 13.528 \pm 0.000$, and $W4 = 9.962 \pm 0.000$), and WISE J080310.27–685536.4 ($W1 = 15.655 \pm 0.034$, $W2 = 14.973 \pm 0.043$, $W3 = 12.407 \pm 0.176$, and $W4 = 9.794 \pm 0.000$);
- SwiftFT J080310.3–6855.5;
- 1SXPS J080310.3–685535.

Due to the poor quality of the X–ray data, we cannot perform a reliable spectral analysis. However, a simple power law passing through Galactic absorption ($N_{\rm H(Gal)} = 1.18 \times 10^{21}$ cm^{-2}) provides a good fit to the data, yielding a photon index $\Gamma = \left(1.87^{+0.71}_{-0.66}\right)$ and a 2–10 keV flux of $\sim 7 \times 10^{-14}$ erg cm^{-2} s^{-1}.

➢ Source #2, which lies within the 99% IBIS error circle, is located at:

R.A.(J2000) = $08^{\rm h}03^{\rm m}53'.40$

Dec.(J2000) = $-68^{\circ}56'08''.50$

error box = $6''.00$

It is detected at 4.5σ c.l. in the 0.3–10 keV energy band, but not above 3 keV.

Multi–wavelength counterparts to this XRT detection:

- USNO–A2.0 U0150.05121126 ($R = 7.0$), and USNO–A2.0 U0150.05121093 ($R = 11.1$, and $B = 11.5$);
- 2MASS J08035322–6856126 with magnitudes $J = 5.247 \pm 0.037$, $H = 4.924 \pm 0.076$, and $K = 4.601 \pm 0.016$;
- WISE J080353.20–685612.5 with colours $W1 = 4.546 \pm 0.091$, $W2 = 4.210 \pm 0.048$, $W3 = 4.565 \pm 0.014$, and $W4 = 4.526 \pm 0.021$;
- 1SXPS J080353.5–685612;
- Star HD 67624 of spectral type G6III.

➢ Source #3, which lies at the border of the 99% IBIS error circle, is located at:

R.A.(J2000) = $08^{\rm h}01^{\rm m}47'.70$

Dec.(J2000) = $-68^{\circ}52'04''.80$

error box = $6''.00$

It is detected in the 0.3–10 keV energy band at 5.2σ c.l., and is still observed at energies above 3 keV at 3.2σ c.l.

Multi–wavelength counterparts to this XRT detection:

- USNO–A2.0 U0150.05103866 with magnitudes $R = 15.2$, and $B = 15.4$;
- 2MASS J08014772–6852087 with magnitudes $J = 15.979 \pm 0.143$, $H = 15.410 \pm 0.192$, and $K = 14.581 \pm 0.126$;
- WISE J080147.71–685208.7 with colours $W1 = 13.742 \pm 0.024$, $W2 = 13.428 \pm 0.025$, $W3 = 11.210 \pm 0.060$, and $W4 = 8.446 \pm 0.121$;
- SwiftFT J080147.9–6852.0;
- 1SXPS J080147.8–685208.

The X–ray data are modelled with a simple power law ($N_{\mathrm{H}(Gal)} = 1.18 \times 10^{21}$ cm^{-2}), with a flat photon index $\Gamma = \left(0.34^{+0.58}_{-0.75}\right)$ and a 2–10 keV flux of $\sim 3 \times 10^{-13}$ erg cm^{-2} s^{-1}.

This is another case in which the X–ray data prevent us from pinpointing the likely counterpart. Source #1 might be a likely candidate because of its location within the 90% IBIS error circle, but only optical follow–up observations will confirm this suggestion.

SWIFT J0924.2–3141

(IBIS detection: persistent)

Three XRT observations available:

1. obscode: 00091688001
   observation date: 02/04/2013
   exposure: 2596 s
2. obscode: 00091688002
   observation date: 07/04/2013
   exposure: 2384 s
3. obscode: 00080674001
   observation date: 19/04/2014
   exposure: 6650 s

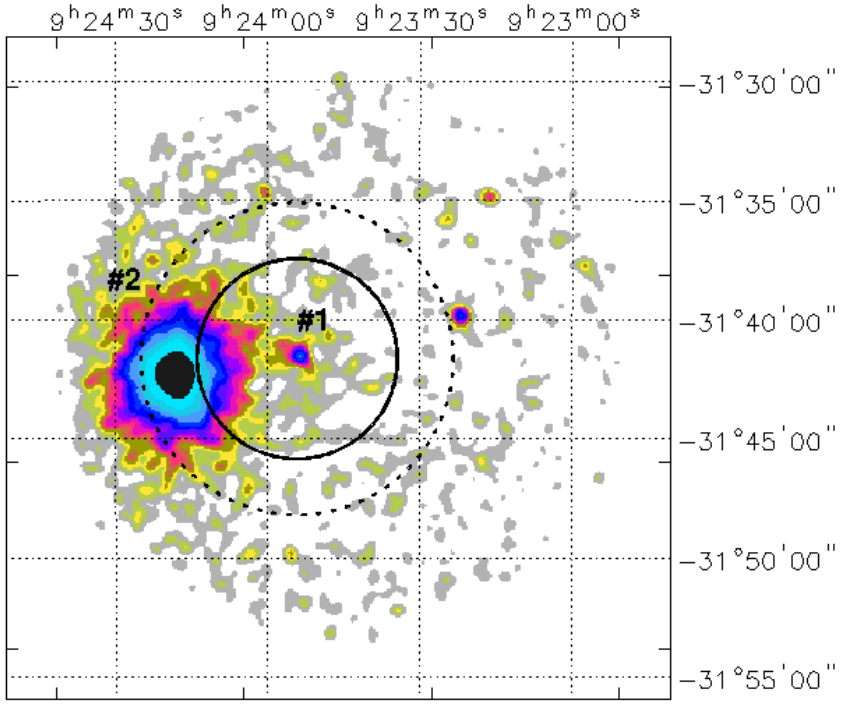

Figure 9: 0.3–10 keV XRT image of the 1RXS J092418.0–3141 field.

XRT detects two X–ray sources, whose positions are compatible with either the 90% or the 99% IBIS positional uncertainty:

➢ Source #1, which lies within the 90% IBIS error circle, is located at:

R.A.(J2000) = $09^h23^m53'.50$

Dec.(J2000) = $-31^\circ 41' 30''.20$

error box = $6''.00$

It is detected at 6.6σ and 6.4σ c.l. in 0.3–10 keV energy range and above 3 keV, respectively. The source is visible at 2.3σ c.l. up to 6.7 keV.

Multi–wavelength counterparts to this XRT detection:

- USNO–A2.0 U0525.11601717 with magnitudes $R = 11.7$, and $B = 12.9$;
- 2MASS J09235373–3141308 with magnitudes $J = 14.242 \pm 0.087$, $H = 13.515 \pm 0.103$, and $K = 12.979 \pm 0.071$;
- WISE J092353.73–314130.9 with colours $W1 = 11.948 \pm 0.023$, $W2 = 11.532 \pm 0.022$, $W3 = 9.141 \pm 0.029$, and $W4 = 6.825 \pm 0.068$;
- NVSS J092353–314126 (F(1.4 GHz) = 4.4 ± 0.5 mJy);
- This source has been proposed as the counterpart of SWIFT J0924.2–3141 (Baumgartner et al. 2013). It is classified as a Seyfert 1.8 at $z = 0.042$ in the Veron & Veron (13^{th} edition) catalogue.

The X–ray data, although of poor statistical quality, seems to require a double power law model, with the primary component absorbed by intrinsic absorption and the secondary component, having the same photon index (frozen to 1.8) of the primary one, passing only through the Galactic column density ($N_{\rm H(Gal)} = 1.33 \times 10^{21}$ cm^{-2}). The intrinsic absorption, albeit poorly constrained, is found to be around 8×10^{23} cm^{-2}; the 2–10 keV flux is $\sim 1.3 \times 10^{-12}$ erg cm^{-2} s^{-1}.

➢ Source #2, which lies within the 99% IBIS error circle, is located at:

R.A.(J2000) = $09^{\rm h}24^{\rm m}18'.18$

Dec.(J2000) = $-31^\circ 42' 17''.97$

error box = $3''.51$

It is detected at 152σ and 83σ c.l. in the 0.3–10 keV energy band and above 3 keV, respectively.

Multi–wavelength counterparts to this XRT detection:

- USNO–A2.0 U0525.11615396 with magnitudes $R = 17.3$, and $B = 19.2$;
- CXO J092418.2–314217;
- SAXWFC J0924.3–3142.4;
- *ROSAT* Bright source 1RXS J092418.0–314212 (0.4 arcseconds error radius);
- XMMSL1 J092418.4–314219 with a 0.2–12 keV flux of $\sim 1.42 \times 10^{-10}$ erg cm^{-2} s^{-1}.

By fitting the average XRT spectrum with a simple power law ($N_{\rm H(Gal)} = 1.32 \times 10^{21}$ cm^{-2}), we found a photon index $\Gamma = (1.39 \pm 0.03)$ and a 2–10 keV flux of $\sim$2.4 $\times$ 10^{-10} erg cm^{-2} s^{-1}. The addition of a blackbody component provides a significant improvement of the fit ($\Delta\chi^2 = 40.0/2$), yielding a temperature $kT = 1.16 \pm 0.10$ keV, a photon index $\Gamma = (1.66 \pm 0.03)$ and a 2–10 keV flux of $\sim$2.4 $\times$ 10^{-10} erg cm^{-2} s^{-1}.

This source shows a flux variability by a factor of 1.7 over a year time. It is also reported as a *HEAO–1* A3 MC LASS source (H0922–374), where it is classified as an X–ray binary in the Galaxy. Apparently, the X–ray flux is far too bright for an AGN of magnitude $V \sim 21$. The X–ray/optical fluxes and ASM colours most resamble the low luminosity ultra compact binaries.

Source #1 has been proposed by Baumgartner et al. (2013) as the counterpart to SWIFT J0924.2–3141. As can be seen in Figure 9, the XRT data show a more complex situation in the region surrounding the IBIS detection. One the one hand, even though source #2 is located outside the IBIS positional uncertainty, its brightness in X–ray, which has been found to be a factor of 100 higher that that of source #1, suggests a significant contribution to the high–energy emission. On the other hand, source #1 lies within the IBIS error circle, implying that its contribution to the IBIS emission cannot be neglected. Indeed, from the XRT image analysis we found that source #1 is detected in X–ray up to around 7 keV.

IGR J12107+0525

(IBIS detection: 0.5–day outburst)

Eleven XRT observations available:

1. obscode: 00091294001
   observation date: 03/08/2012
   exposure: 7600 s

2. obscode: 00091294002
   observation date: 15/11/2012
   exposure: 1437 s

3. obscode: 00091294003
   observation date: 16/11/2012
   exposure: 586 s

4. obscode: 00091294004
   observation date: 20/11/2012
   exposure: 750 s

5. obscode: 00091294005
   observation date: 25/01/2013
   exposure: 216 s

6. obscode: 00091294007
   observation date: 01/03/2013
   exposure: 1016 s

7. obscode: 00091664001
   observation date: 12/11/2013
   exposure: 231 s

8. obscode: 00091664002
   observation date: 23/11/2013
   exposure: 5158 s

9. obscode: 00091664003
   observation date: 24/01/2014
   exposure: 524 s

10. obscode: 00091664004
    observation date: 13/02/2014
    exposure: 775 s

11. obscode: 00091664005
    observation date: 14/02/2014
    exposure: 774 s

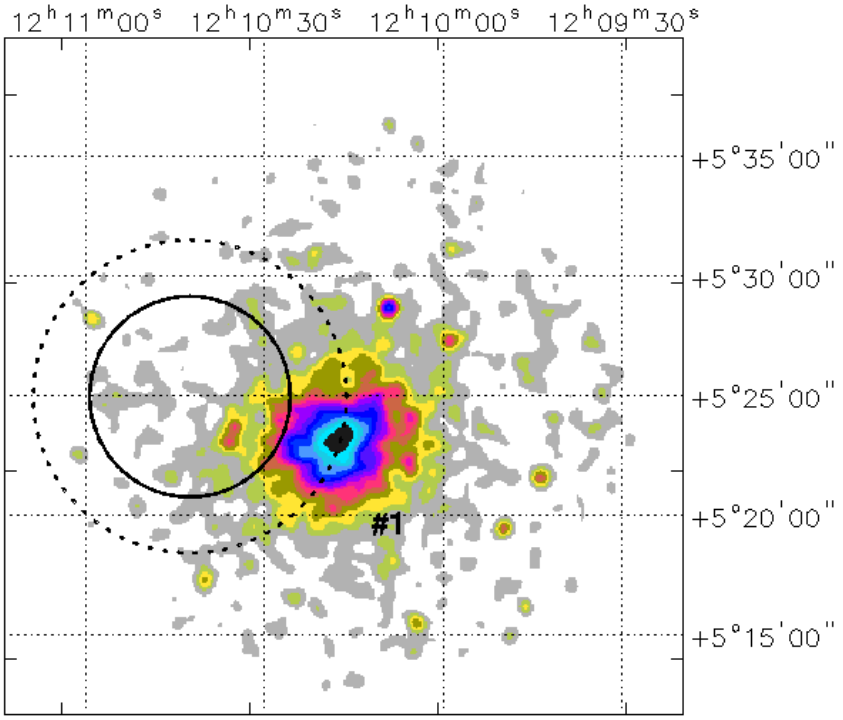

Figure 10: 0.3–10 keV XRT image of the IGR J12107+0525 field.

XRT detects a diffuse emission, compatible with the 99% IBIS positional uncertainty, which coincides with the cluster of galaxies ZWCl 1207+0542. The brightest XRT detection lies at 0.′213 from the centre of the Cluster and is located at:

R.A.(J2000) = $12^h10^m16'.40$

Dec.(J2000) = $+05°23'20''.90$

error box = $6''.00$

It is detected at 15σ c.l. in the 0.3–10 keV energy range, and it is still detected above 3 keV at 6.7σ c.l.

The brightes galaxy in the cluster is located at:

R.A.(J2000) = $12^h10^m16'.791$

Dec.(J2000) = $+05°23'09''.75$

just at the core of the cluster. It has a $z = 0.076162$. Its optical spectrum displays only [NII]$\lambda\lambda$ 6548 line emission.

This in another case in which no firm conclusions can be drawn from the X–ray data, as the cluster is highly unlikely to provide variable emission as observed by IBIS.

IGR J12207+1517

(IBIS detection: 1398.9–day outburst)

Three XRT observations available:

1. obscode: 00048099002
   observation date: 31/07/2012
   exposure: 4634 s
2. obscode: 00048099003
   observation date: 02/08/2012
   exposure: 426 s
3. obscode: 00048099004
   observation date: 03/08/2012
   exposure: 2588 s

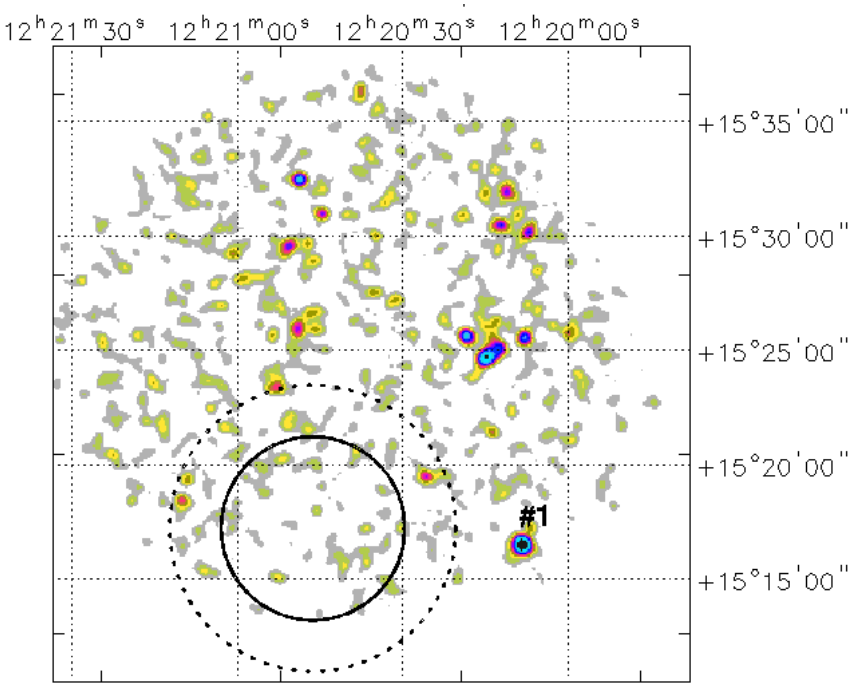

Figure 11: 0.3–10 keV XRT image of the IGR J12207+1517 field.

No source is detected by XRT within both the 90% and 99% IBIS error circles. There is an X–ray detection at around 3 arcminutes from the border of the 99% IBIS positional uncertainty located at:

R.A.(J2000) = $12^h20^m08'.36$

Dec.(J2000) = $+15°16'29''.15$

error box = $4''.69$

It is detected at 6.4σ c.l. in 0.3–10 keV energy band, and it is not observed above 3 keV.

Multi–wavelength counterparts to this XRT detection:

- USNO–A2.0 U1050.06696988 with magnitudes $R = 17.1$, and $B = 17.4$;
- 2MASS J12200844+1516300 with magnitudes $J = 16.532 \pm 0.124$, $H = 15.842 \pm 0.152$, and $K = 14.788 \pm 0.123$;
- WISE J122008.44+151630.2 with colours $W1 = 13.505 \pm 0.027$, $W2 = 12.485 \pm 0.026$, $W3 = 9.246 \pm 0.031$, and $W4 = 6.591 \pm 0.057$;
- SDSS J122008.44+151630.1 (QSO, $z = 0.222658$);
- 1SXPS J122008.3+151628.

As source #1 lies far from the IBIS positional uncertainty, no contribution to the high-energy emission can be ascribed to this X–ray source, leaving the IBIS detection still unassociated.

IGR J14059–6116

(IBIS detection: 2198.6–day outburst)

One XRT observation available:

1. obscode: 00041805005
   observation date: 21/09/2012
   exposure: 4644 s

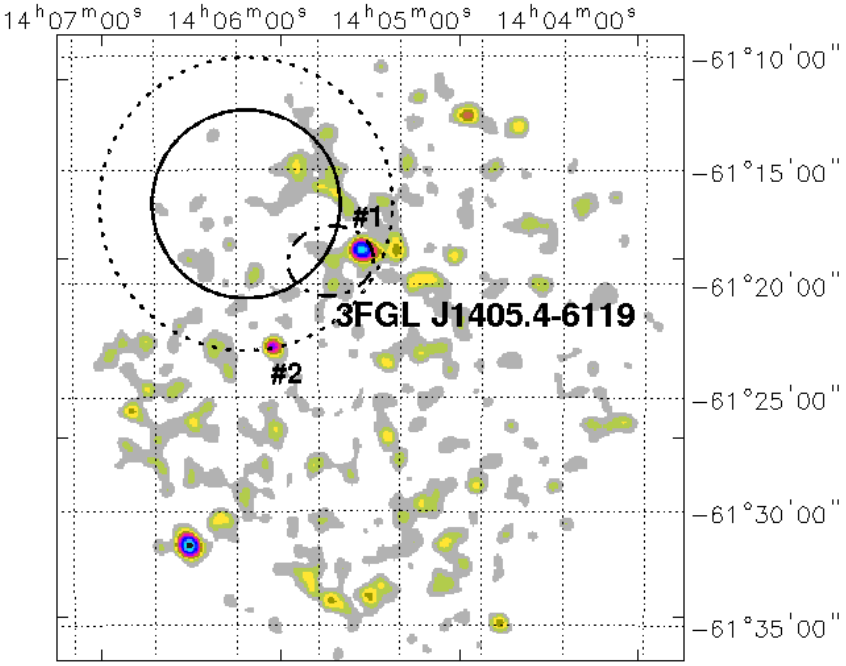

Figure 12: 0.3–10 keV XRT image of the IGR J14059–6116 field. The black–dashed–dotted circle depicts the positional uncertainty of the *Fermi* source 3FGL J1405.4–6119.

There are two X–ray sources whose positions are compatible with the 99% IBIS positional uncertainty:

➢ Source #1 (within the 99% IBIS error circle) is located at:

R.A.(J2000) = $14^{h}05^{m}14'.10$

Dec.(J2000) = $-61°18'28''.90$

error box = $6''.00$

It is detected at 4.5σ and 4.3σ c.l. in the 0.3–10 keV and above 3 keV, respectively.

Multi–wavelength counterparts to this XRT detection:

- USNO–B1.0 0286–0475536 with magnitudes $R1 = R2 = 17.32$, and $B2 = 19.25$;
- 2MASS J14051441–6118282 ($J = 15.962 \pm 0.000$, $H = 14.369 \pm 0.068$, and $K = 12.769 \pm 0.044$), and 2MASS J14051422–6118228 ($J = 15.393 \pm 0.060$, $H = 14.747 \pm 0.070$, and $K = 14.300 \pm 0.084$);
- WISE J140514.41–611827.8 with colours $W1 = 11.675 \pm 0.039$, $W2 = 11.222 \pm 0.048$, $W3 = 9.969 \pm 0.000$, and $W4 = 7.573 \pm 0.000$;
- 1SXPS J140514.2–611828.

This X–ray source has no radio counterpart and its WISE colours ($W1 - W2 = 0.453$, and $W2 - W3 = 1.25$) are not typical of gamma–ray selected blazar. It is worth noticing that this keV/GeV source is located at low Galactic latitude, i.e. on the Galactic plane. The *Fermi* source has been suggested to be associated with a pulsar (Lee et al. 2012).

From the XRT data, we can only infer a 2–10 keV flux roughly around 1×10^{-13} erg cm^{-2} s^{-1}, by assuming a power law model ($N_{\rm H(Gal)} = 1.84 \times 10^{22}$ cm^{-2}) with the photon index frozen to 1.8.

➢ Source #2 (at the border of the 99% IBIS error circle) is located at:

R.A.(J2000) = $14^{\rm h}05^{\rm m}46'.50$

Dec.(J2000) = $-61^\circ 22' 46''.30$

error box = $6''.00$

It is detected at 2.6σ c.l. in the 0.3–10 keV energy band, and it is not revealed above 3 keV.

Multi–wavelength counterparts to this XRT detection:

- USNO–A2.0 U0225.19132548 with magnitudes $R = 15.1$, and $B = 16.6$;
- 2MASS J14054683–6122463 with magnitudes $J = 11.676 \pm 0.024$, $H = 11.048 \pm 0.023$, and $K = 10.790 \pm 0.023$;
- WISE J140546.74–612246.5 with colours $W1 = 10.504 \pm 0.027$, $W2 = 10.307 \pm 0.024$, $W3 = 10.196 \pm 0.000$, and $W4 = 8.802 \pm 0.000$;
- 1SXPS J140546.8–61224.

This is another case in which, at this stage, the X–ray data available prevent us from proposing any likely counterpart to the IBIS detection. However, we note that the positional uncertainty of the still unassociated *Fermi* source 3FGL J1405.4–6119 (Acero et al. 2015) encloses source #1.

IGR J14235–1547

(IBIS detection: persistent)

Six XRT observations available:

1. obscode: 00048096001
   observation date: 24/12/2011
   exposure: 2328 s
2. obscode: 00048096003
   observation date: 29/03/2012
   exposure: 143 s
3. obscode: 00048096004
   observation date: 30/03/2012
   exposure: 258 s
4. obscode: 00048096005
   observation date: 19/04/2012
   exposure: 504 s
5. obscode: 00048096006
   observation date: 07/05/2012
   exposure: 256 s
6. obscode: 0004809600
   observation date: 09/05/2012
   exposure: 1046 s

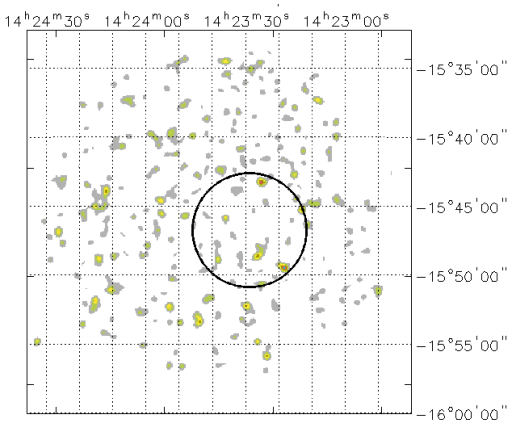

Figure 13: 0.3–10 keV XRT image of the IGR J14235–1547 field.

No source has been detected by XRT within the IBIS error circle, nor in the whole XRT FoV.

IGR J14319–3315

(IBIS detection: 1035.3–day outburst)

One XRT observation available:

1. obscode: 00037072001
   observation date: 26/12/2009
   exposure: 4286 s

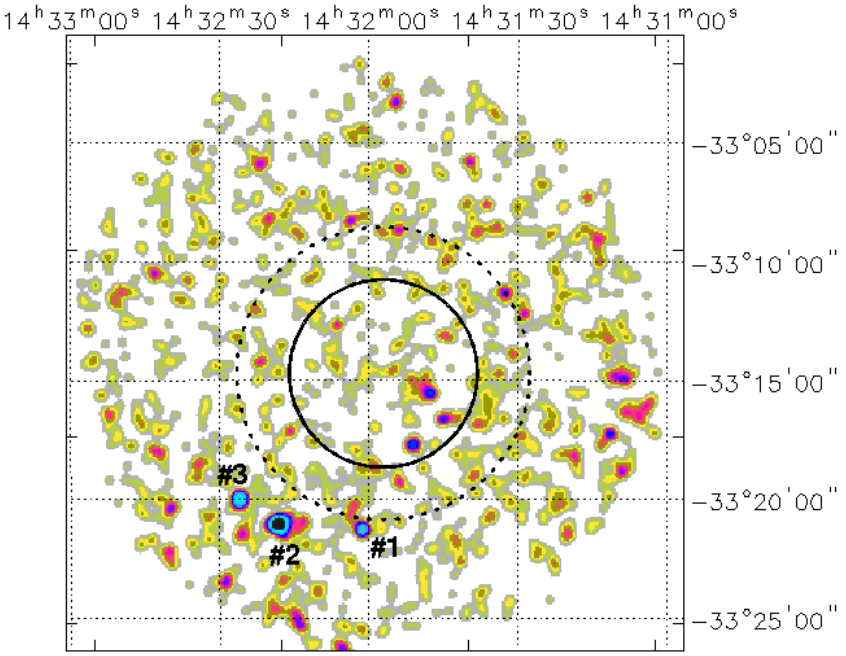

Figure 14: 0.3–10 keV XRT image of the IGR J14319–3315 field.

The three X–ray sources detected by XRT are located outside the 99% IBIS positional uncertainty:

➢ Source #1 is the closest to the 99% IBIS error circle and is located at:

R.A.(J2000) = $14^{h}32^{m}01'.20$

Dec.(J2000) = $-33^{\circ}21'15''.90$

error box = $6''.00$

It is detected at 2.8σ c.l. in the 0.3–10 keV, and it is not observed above 3 keV.

Multi–wavelength counterparts to this XRT detection:

- USNO–A2.0 U0525.17660788 with magnitudes $R = 18.1$, and $B = 19.2$;
- WISE J143201.44–332113.4 with colours $W1 = 16.245 \pm 0.059$, $W2 = 15.402 \pm 0.117$, $W3 = 11.938 \pm 0.235$, and $W4 = 8.753 \pm 0.000$;
- GALEXASC J143201.49–332113.3;
- 1SXPS J143201.3–332117.

➢ Source #2 is located at:

R.A.(J2000) = $14^{\rm h}32^{\rm m}18'.00$

Dec.(J2000) = $-33°21'01''.60$

error box = $6''.00$

It is detected at 6.2σ c.l. in the 0.3–10 keV energy band, and it is not revealed above 3 keV.

Multi–wavelength counterparts to this XRT detection:

- USNO–B1.0 0566–0367548 ($R1 = 12.94$, and $R2 = 13.03$); USNO–B1.0 0566–0367547 ($R1 = 13.20$, $R2 = 0.0$, $B1 = 15.66$, and $B2 = 15.40$);
- 2MASS J14321800–3320588 with magnitudes $J = 9.685 \pm 0.023$, $H = 9.107 \pm 0.023$, and $K = 8.809 \pm 0.020$;
- WISE J143218.13–332059.5 with colours $W1 = 8.677 \pm 0.022$, $W2 = 8.508 \pm 0.021$, $W3 = 8.411 \pm 0.022$, and $W4 = 8.315 \pm 0.255$;
- 1SXPS J143218.0–332101;
- The source is probably a southern red dwarf system.

➢ Source #3 is located at:

R.A.(J2000) = $14^{\rm h}32^{\rm m}26'.00$

Dec.(J2000) = $-33°19'59''.30$

error box = $6''.00$

It is detected at 3.6σ c.l. in the 0.3–10 keV energy band, and it is still detected above 3 keV at 2.2σ c.l.

Multi–wavelength counterparts to this XRT detection:

- USNO–A2.0 U0525.17672265 with magnitudes $R = 15.7$, and $B = 16.8$;

- 2MASS J14322613–3319586 with magnitudes $J = 14.946 \pm 0.033$, $H = 14.566 \pm 0.029$, and $K = 14.505 \pm 0.097$;
- WISE J143226.13–331958.4 with colours $W1 = 14.535 \pm 0.028$, $W2 = 14.620 \pm 0.070$, $W3 = 12.826 \pm 0.000$, and $W4 = 8.778 \pm 0.000$;
- 1SXPS J143226.0–331959.

Also in this case, taking into account information collected from the XRT data, none of the X–ray detections which has been found in the region surrounding IGR J14319–3315 is a likely association.

IGR J14443–2750

(IBIS detection: 9.1–day outburst)

Three XRT observations available:

1. obscode: 000342121000
   observation date: 05/02/2009
   exposure: 29986 s

2. obscode: 000342121003
   observation date: 07/02/2009
   exposure: 8262 s

3. obscode: 000342121004
   observation date: 08/02/2009
   exposure: 18922 s

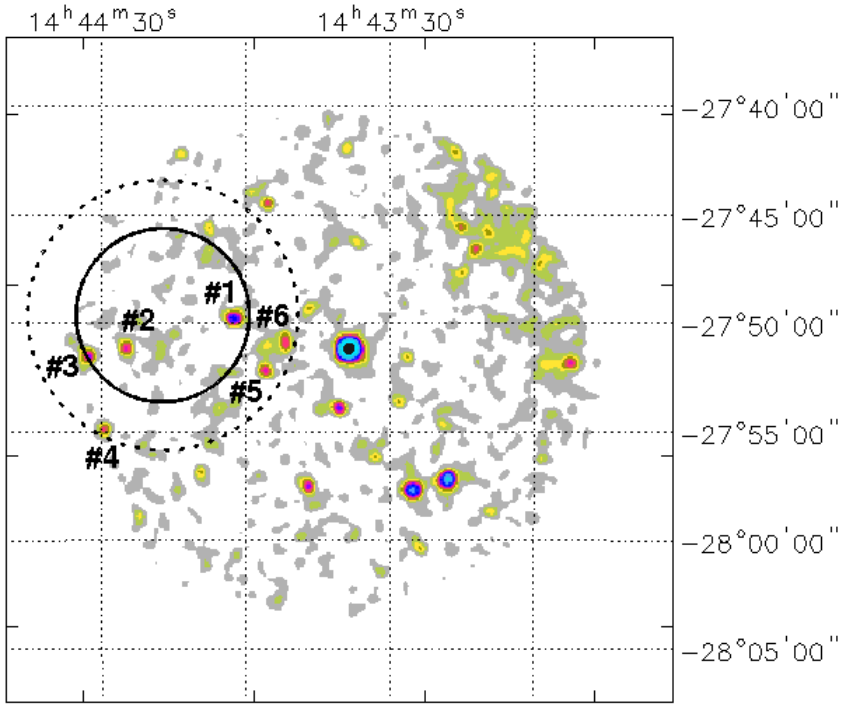

Figure 15: 0.3–10 keV XRT image of the IGR J14443–2750 field.

There are six X–ray sources detected in either the 90% or the 99% IBIS error circles:

➢ Source #1, which is found within the 90% IBIS error circle, is located at:

R.A.(J2000) = $14^h44^m02'.40$

Dec.(J2000) = $-27^{\circ}49'47''.40$

error box = $6''.00$

It is detected at 6.5σ and 3.5σ c.l. in the 0.3–10 keV and above 3 keV, respectively.

Multi–wavelength counterparts to this XRT detection:

- WISE J144402.19–274951.0 with colours $W1 = 16.766 \pm 0.097$, $W2 = 15.986 \pm 0.251$, $W3 = 12.167 \pm 0.312$, and $W4 = 8.892 \pm 0.000$;
- 1SXPS J144402.5–274948.

By modelling the XRT data with a power law passing through Galactic absorption ($N_{\rm H(Gal)} = 7.83 \times 10^{20}$ cm^{-2}), we find a flat photon index $\Gamma \sim 1.1$ and a 2–10 keV flux of $\sim 7 \times 10^{-14}$ erg cm^{-2} s^{-1}.

➢ Source #2, which lies within the 90% IBIS error circle, is located at:

R.A.(J2000) = $14^{\rm h}44^{\rm m}24'.70$

Dec.(J2000) = $-27^{\circ}51'08''.00$

error box = $6''.00$

It is detected at 4.9σ c.l. in the 0.3–10 keV energy band, and it is not revealed above 3 keV.

Multi–wavelength counterparts to this XRT detection:

- 1SXPS J144424.7–275107.

➢ Source #3, which is found at the border of the 90% IBIS error circle, is located at:

R.A.(J2000) = $14^{\rm h}44^{\rm m}32'.70$

Dec.(J2000) = $-27^{\circ}51'27''.90$

error box = $6''.00$

It is detected at 5.9σ c.l. in the 0.3–10 keV energy band, and it is not revealed above 3 keV.

Multi–wavelength counterparts to this XRT detection:

- WISE J144433.20–275129.0 with colours $W1 = 15.807 \pm 0.054$, $W2 = 15.296 \pm 0.125$, $W3 = 12.764 \pm 0.495$, and $W4 = 8.903 \pm 0.000$;

- 1SXPS J144433.0–275130.

➢ Source #4, which is detected within the 99% IBIS error circle, is located at:

R.A.(J2000) = $14^{\rm h}43^{\rm m}51'.60$

Dec.(J2000) = $-27^{\circ}50'50''.30$

error box = $6''.00$

It is detected at 4.6σ c.l. in the 0.3–10 keV energy band, and it is not revealed above 3 keV.

Multi–wavelength counterparts to this XRT detection (at around 8 arcseconds):

- USNO–B1.0 0621–0395999 with magnitudes $R1 = 14.18$, $R2 = 14.61$, $B1 = 16.58$, and $B2 = 15.90$;
- 2MASS J14435193–2750573 with magnitudes $J = 13.009 \pm 0.026$, $H = 12.316 \pm 0.024$, and $K = 12.175 \pm 0.028$;
- WISE J144351.94–275057.2 with colours $W1 = 12.045 \pm 0.022$, $W2 = 12.167 \pm 0.025$, $W3 = 12.241 \pm 0.328$, and $W4 = 9.094 \pm 0.000$;
- 1SXPS J144351.6–275040.

➢ Source #5, which lies within the 99% IBIS error circle, is located at:

R.A.(J2000) = $14^{\rm h}43^{\rm m}55'.80$

Dec.(J2000) = $-27^{\circ}52'10''.70$

error box = $6''.00$

It is detected at 4.6σ c.l. in the 0.3–10 keV energy band, and it is not revealed above 3 keV.

Multi–wavelength counterparts to this XRT detection:

- 1SXPS J144355.8–275212.

➢ Source #6, which is detected within the 99% IBIS error circle, is located at:

R.A.(J2000) = $14^{\rm h}44^{\rm m}29'.30$

Dec.(J2000) = $-27^{\circ}54'52''.80$

error box = $6''.00$

It is detected at 4.6σ c.l. in the 0.3–10 keV energy band, and it is not revealed above 3 keV.

Multi–wavelength counterparts to this XRT detection:

- USNO–A2.0 U0600.17114247 with magnitudes $R = 18.1$, and $B = 19.1$;
- WISE J144429.49–275456.4 with colours $W1 = 15.818 \pm 0.051$, $W2 = 14.534 \pm 0.064$, $W3 = 11.978 \pm 0.229$, and $W4 = 8.746 \pm 0.349$;
- GALEXASC J144429.50–275455.9;
- 1SXPS J144429.4–275454.

On the basis of the characteristics found for each XRT detection, there is no clear evidence of a likely counterpart, although source #1, being the only X–ray object detected above 3 keV, may be a good candidate, expecially in view of the variability of the IBIS flux.

IGR J15038–6021

(IBIS detection: persistent)

Two XRT observations available:

1. obscode: 00046303001
   observation date: 12/05/2013
   exposure: 354 s

2. obscode: 00046303002
   observation date: 07/04/2013
   exposure: 1309 s

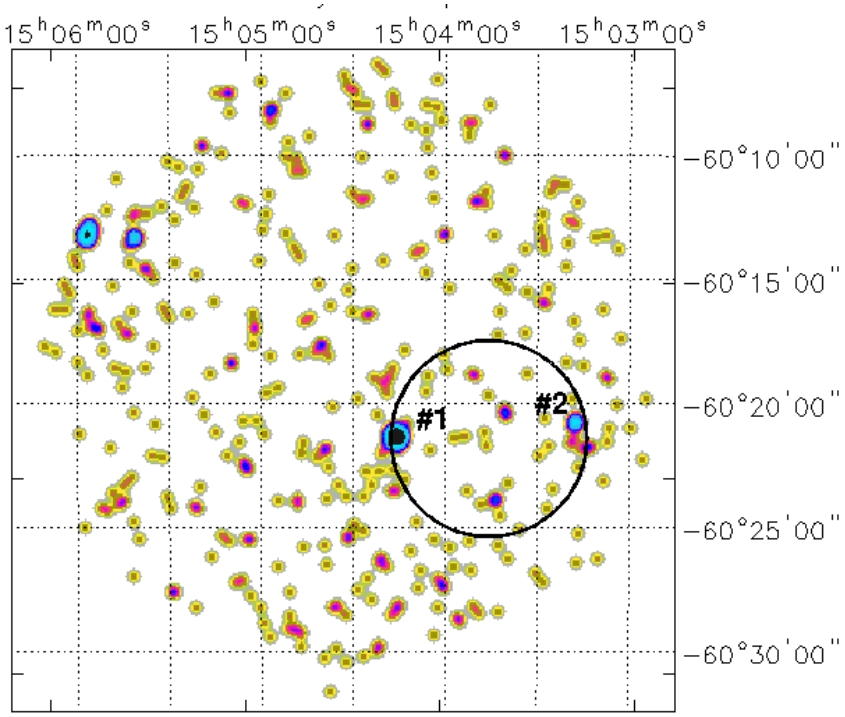

Figure 16: 0.3–10 keV XRT image of the IGR J15038–6021 field.

XRT detects two X–ray sources whose positions are compatible with the 90% IBIS positional uncertainty:

➢ Source #1, which lies at the border of the 90% IBIS error circle, is located at:

R.A.(J2000) = $15^{h}04^{m}15'.99$

Dec.(J2000) = $-60°21'21''.62$

error box = $5''.11$

It is detected at 6.2σ c.l. in the 0.3–10 keV energy band, and it is still visible above 3 keV at 4.1σ c.l.

Multi–wavelength counterparts to this XRT detection:

- USNO–B1.0 0296–0547603 ($R1 = 17.77$, and $R2 = 19.04$), and USNO–B1.0 0296–0547602 ($R2 = 18.63$);
- 2MASS J15041611–6021225 with magnitudes $J = 15.824 \pm 0.000$, $H = 14.594 \pm 0.000$, and $K = 14.629 \pm 0.106$.

Although, because of the low statistical quality of the data, the spectral parameters are poorly constrained, the X–ray spectrum can be modelled with a power law ($N_{\rm H(Gal)} = 1.26 \times 10^{22}$ cm^{-2}) having a photon index Γ around 1.9 and a 2–10 keV flux of $\sim 1.3 \times 10^{-12}$ erg cm^{-2} s^{-1}.

➢ Source #2, which lies at the border of the 90% IBIS error circle, is located at:

R.A.(J2000) = $15^{\rm h}03^{\rm m}17'.60$

Dec.(J2000) = $-60^\circ 20' 45''.70$

error box = $6''.00$

It is detected at 2.6σ in the 0.3–10 keV energy range, but not above 3 keV.

No multi–wavelength counterparts has been found to this XRT detection:

In this case, the X–ray data suggest that source #1 could be a likely counterpart to IGR J15038–6021.

IGR J16181–5407

(IBIS detection: persistent)

Twelve XRT observations available:

1. obscode: 00045375001
   observation date: 07/07/2011
   exposure: 658 s

2. obscode: 00045375002
   observation date: 30/08/2011
   exposure: 720 s

3. obscode: 00045375003
   observation date: 22/07/2011
   exposure: 403 s

4. obscode: 00045375005
   observation date: 11/04/2013
   exposure: 1028 s

5. obscode: 00045375006
   observation date: 16/04/2013
   exposure: 1657 s

6. obscode: 00045375007
   observation date: 17/07/2013
   exposure: 359 s

7. obscode: 00045375010
   observation date: 07/05/2013
   exposure: 273 s

8. obscode: 00045375012
   observation date: 16/05/2013
   exposure: 552 s

9. obscode: 00045375013
   observation date: 18/05/2013
   exposure: 577 s

10. obscode: 00045375014
    observation date: 20/05/2013
    exposure: 616 s

11. obscode: 00045375015
    observation date: 23/05/2013
    exposure: 774 s

12. obscode: 00045375016
observation date: 25/05/2013
exposure: 710 s

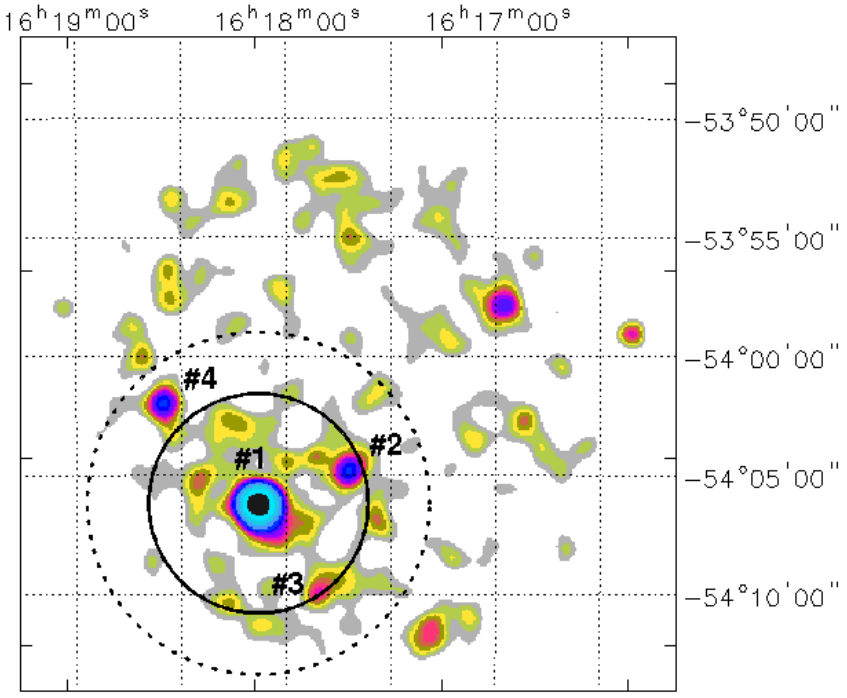

Figure 17: 0.3–10 keV XRT image of the IGR J16181–5407 field.

There are four X–ray sources whose positions are compatible with either the 90% or the 99% IBIS positional uncertainties:

➢ Source #1, which lies within the 90% IBIS error circle, is located at:

R.A.(J2000) = $16^h18^m07'.75$

Dec.(J2000) = $-54°06'14''.52$

error box = $3''.81$

It is detected at 14.2σ c.l. in 0.3–10 keV energy band, and it is still observed above 3 keV at 13.2σ c.l.

Multi–wavelength counterparts to this XRT detection:

- USNO–A2.0 U0300.27714197 with magnitude $R = 16.6$, and $B = 18.2$;

- 2MASS J16180771–5406122 ($J = 14.170 \pm 0.000$, $H = 14.091 \pm 0.083$, and $K = 12.854 \pm 0.063$), 2MASS J16180744–5406117 ($J = 14.768 \pm 0.072$, $H = 13.501 \pm 0.000$, and $K = 12.769 \pm 0.000$), and 2MASS J16180824–5406105 ($J = 14.344 \pm 0.061$, $H = 13.679 \pm 0.073$, and $K = 13.445 \pm 0.059$)[1];
- WISE J161807.76–540612.3 with colours $W1 = 11.312 \pm 0.038$, $W2 = 10.097 \pm 0.025$, $W3 = 7.546 \pm 0.023$, and $W4 = 4.985 \pm 0.041$;
- 1SXPS J161808.2–540610 (6 arcseconds away from the XRT centroid).

The XRT spectrum is well modelled with an absorbed power law ($N_{\rm H(Gal)} = 5.75 \times 10^{21}$ cm^{-2}); $N_{\rm H(int)} = \left(7.09^{+4.56}_{-2.98}\right) \times 10^{22}$ cm^{-2}) having photon index $\Gamma = \left(1.59^{+0.97}_{-0.79}\right)$ and 2–10 keV flux of $\sim$3.9 $\times 10^{-12}$ erg cm^{-2} s^{-1}.

➢ Source #2, which is detected within the 90% IBIS error circle, is located at:

R.A.(J2000) = $16^{\rm h}17^{\rm m}41'.70$

Dec.(J2000) = $-54^\circ 04' 47''.50$

error box = $6''.00$

It is detected at 3.9σ in the 0.3–10 keV energy band; no detection is observed above 3 keV.

Multi–wavelength counterparts to this XRT detection:

- USNO–A2.0 U0300.27664390 with magnitudes $R = 13.8$, and $B = 16.2$;
- 2MASS J16174152–5404495 ($J = 13.976 \pm 0.510$, $H = 13.218 \pm 0.061$, and $K = 13.018 \pm 0.044$), and 2MASS J16174203–5404482 ($J = 11.243 \pm 0.024$, $H = 10.543 \pm 0.028$, and $K = 10.305 \pm 0.026$);
- WISE J161742.01–540448.3 with colours $W1 = 9.936 \pm 0.023$, $W2 = 10.036 \pm 0.023$, $W3 = 9.889 \pm 0.063$, and $W4 = 8.642 \pm 0.360$.

Given the poor quality of the XRT data, we can only infer a 2–10 keV flux of $\sim 7 \times 10^{-14}$ erg cm^{-2} s^{-1}, by assuming a power law continuum (photon index frozen to 1.8) passing through the Galactic absorption ($N_{\rm H(Gal)} = 5.96 \times 10^{21}$ cm^{-2}).

➢ Source #3, which is detected at the border of the 90% IBIS error circle, is located at:

R.A.(J2000) = $16^{\rm h}17^{\rm m}51'.50$

Dec.(J2000) = $-54^\circ 09' 56''.50$

error box = $6''.00$

[1]This IR counterpart is 6 arcseconds away from the XRT centroid.

It is detected at 2.7σ c.l. in 0.3–10 keV energy band, and is not observed above 3 keV.

Multi–wavelength counterparts to this XRT detection:

- USNO–B1.0 0358–0590670 ($R1 = 18.78$, $R2 = 18.88$, and $B2 = 17.34$), USNO–B1.0 0358–0590654 ($R2 = 18.62$, and $B2 = 17.87$), USNO–B1.0 0358–0590649 ($R1 = 17.61$, and $B2 = 18.79$), and USNO–B1.0 0358–0590722 ($R1 = 15.67$, and $B2 = 17.27$);
- 2MASS J16175191–5409520 with magnitudes $J = 15.009 \pm 0.688$, $H = 14.473 \pm 0.452$, and $K = 13.907 \pm 0.321$;
- WISE J161752.21–540959.2 with colours $W1 = 7.889 \pm 0.023$, $W2 = 7.954 \pm 0.018$, $W3 = 7.997 \pm 0.022$, and $W4 = 8.182 \pm 0.000$.
- Star HD 146243.

From the X–ray data we can only infer a 2–10 keV flux of $\sim 1 \times 10^{-14}$ erg cm^{-2} s^{-1}, by assuming a power law ($N_{\rm H(Gal)} = 5.63 \times 10^{21}$ cm^{-2}) having the photon index frozen to 1.8.

➢ Source #4, which is detected inside the 99% IBIS error circle, is located at:

R.A.(J2000) = $16^{\rm h}18^{\rm m}35'.10$

Dec.(J2000) = $-54^{\circ}01'51''.00$

error box = $6''.00$

It is detected at 4.1σ and 2.6σ c.l. in 0.3–10 keV energy band and above 3 keV, respectively.

Multi–wavelength counterparts to this XRT detection:

- USNO–A2.0 U0300.27765446 with magnitudes $R = 16.9$, and $B = 19.9$;
- 2MASS J16183438–5401528 with magnitudes $J = 15.338 \pm 0.051$, $H = 14.946 \pm 0.067$, and $K = 15.488 \pm 0.000$.

The XRT data are well fitted with a power law passing only through the Galactic absorption ($N_{\rm H(Gal)} = 5.83 \times 10^{21}$ cm^{-2}), yielding a photon index $\Gamma = (1.35 \pm 0.96)$ and a 2–10 keV flux around 2×10^{-13} erg cm^{-2} s^{-1}.

Information collected with the XRT follow–up observations leads us to propose source #1 as the likely counterpart to IGR J16181–5407

IGR J17472+0701

(IBIS detection: 218.5-day outburst)

One XRT observation available:

1. obscode: 00037075001
   observation date: 02/11/2008
   exposure: 4524 s

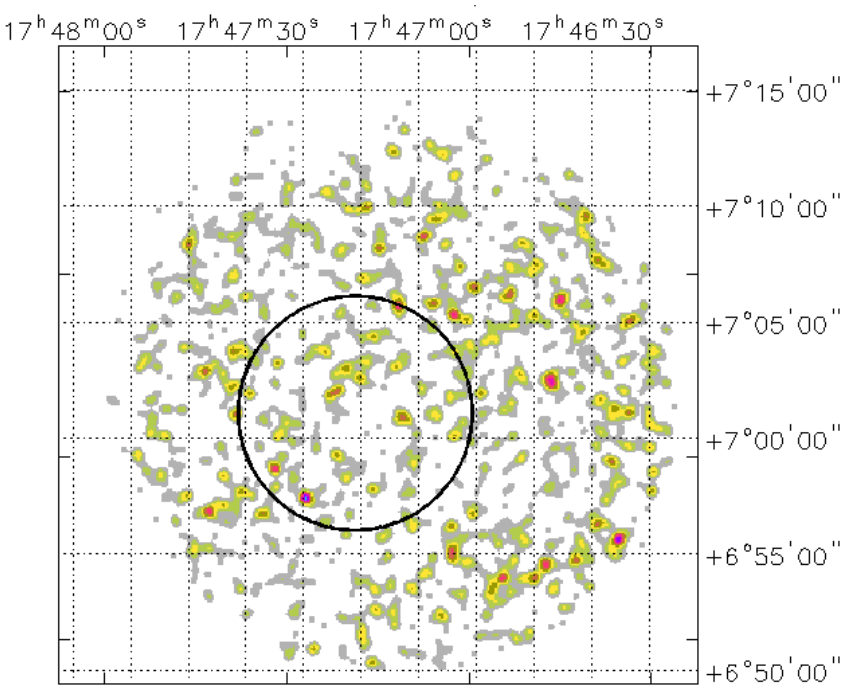

Figure 18: 0.3–10 keV XRT image of the IGR J17472+0701 field, nor in the whole XRT FoV.

No X–ray source has been found within the IBIS error circle.

IGR J18241–1456

(IBIS detection: persistent)

One XRT observation available:

1. obscode: 00044155001
   observation date: 16/10/2012
   exposure: 488 s

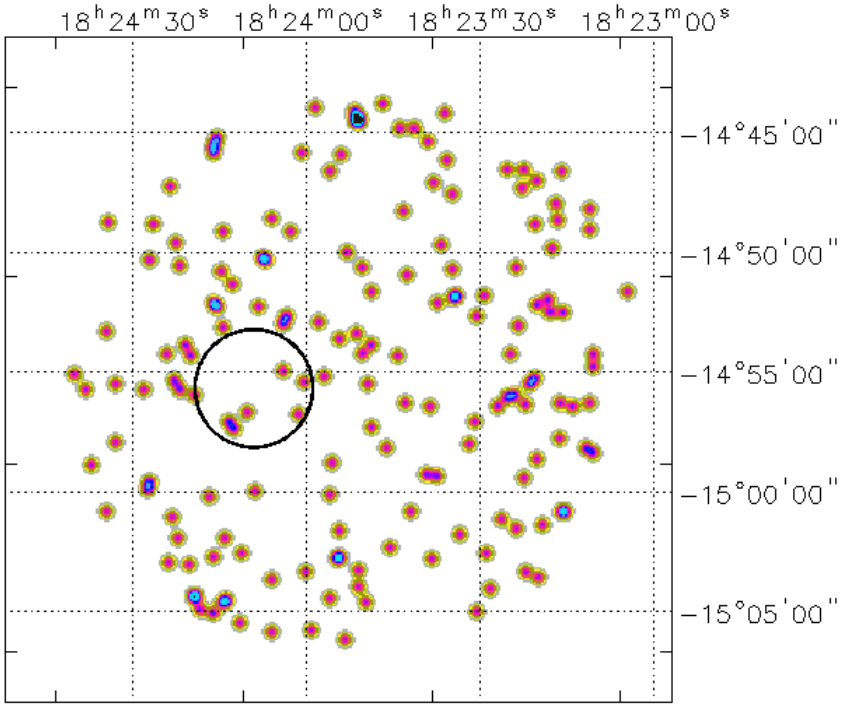

Figure 19: 0.3–10 keV XRT image of the IGR J18241–1456 field, nor in the whole XRT FoV.

No X–ray source has been found within the IBIS error circle, maybe due to the low exposure.

XMMSL1 J182831.3–022901 (PBC J1828.7–0227)

(IBIS detection: persistent)

Eight XRT observations available:

1. obscode: 00049376001
   observation date: 09/11/2012
   exposure: 168 s
2. obscode: 00049376002
   observation date: 12/11/2012
   exposure: 9.4 s
3. obscode: 00049376003
   observation date: 09/02/2012
   exposure: 433 s
4. obscode: 00049376004
   observation date: 23/05/2013
   exposure: 421 s
5. obscode: 00049376005
   observation date: 13/06/2013
   exposure: 201 s
6. obscode: 00049376006
   observation date: 13/06/2013
   exposure: 115 s
7. obscode: 00049376007
   observation date: 19/06/2013
   exposure: 273 s
8. obscode: 00049376008
   observation date: 21/06/2013
   exposure: 3751 s

XRT detects a bright source within the 90% IBIS error circle. It is located at:

R.A.(J2000) = $18^{\rm h}28^{\rm m}31'.09$

Dec.(J2000) = $-02^\circ 29' 06''.66$

error box = $3''.89$

It is detected at 13σ and 10.5σ c.l. in the 0.3–10 keV energy band and above 3 keV, respectively.

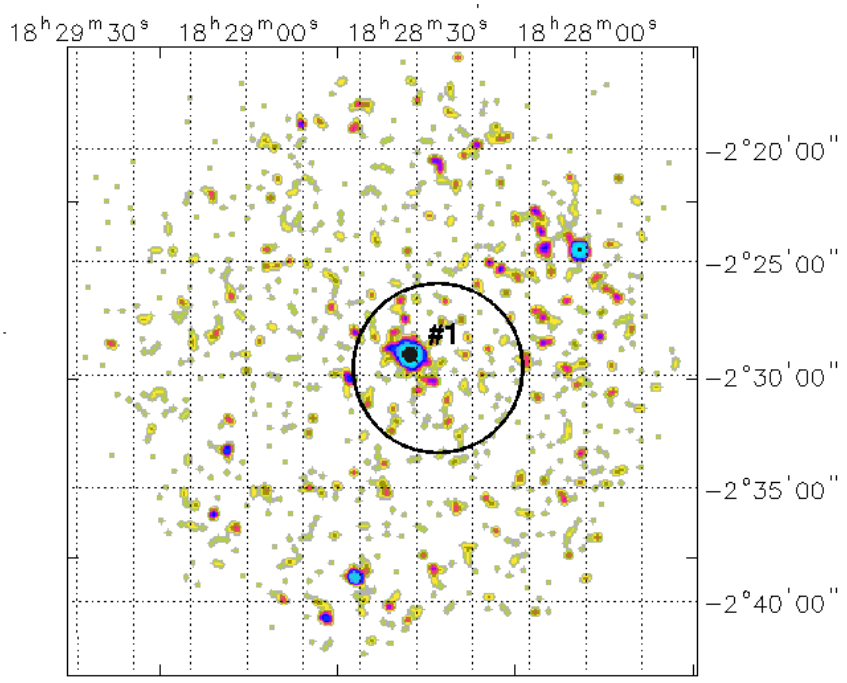

Figure 20: 0.3–10 keV XRT image of the PBC 1828.7–0227 field.

Multi–wavelength counterparts to this XRT detection:

- USNO–B1.0 0875–0521739 with magnitudes $R1 = 17.56$, and $R2 = 17.55$ ($\sim$5 arcseconds away from the XRT centroid);
- 2MASS J18283084–0229086 with magnitudes $J = 16.534 \pm 0.205$, $H = 15.175 \pm 0.130$, and $K = 14.839 \pm 0.204$ ($\sim$5 arcseconds away from the XRT centroid);
- WISE J182831.35–022903.8 with colours $W1 = 9.542 \pm 0.023$, $W2 = 9.573 \pm 0.019$, $W3 = 9.734 \pm 0.064$, and $W4 = 8.301 \pm 0.268$ ($\sim$5 arcseconds away from the XRT centroid);
- XMMSL1 J182831.4–022914 (9.84 arcseconds away from the XRT centroid) with a 0.2–12 keV flux of $\sim 2.3 \times 10^{-12}$ erg cm^{-2} s^{-1}.

This source is located within the massive young star forming complex W40.

The XRT data fitted with a power law passing only through the Galactic absorption ($N_{\rm H(Gal)} = 5.12 \times 10^{21}$ cm^{-2}) do not provide a good fit, which require an additional intrinsic absorption ($N_{\rm H(intr)} = \left(1.53^{+1.34}_{-0.98}\right) \times 10^{22}$ cm^{-2}). The photon index turns out to be $\left(1.21^{+0.75}_{-0.66}\right)$ and the 2–10 keV flux is around 4.6×10^{-12} erg cm^{-2} s^{-1}, which suggests some variability if compared to the *XMM–Newton* one.

SWIFT J1839.1+5717

(IBIS detection: persistent)

Two XRT observations available:

1. obscode: 00038080001
   observation date: 17/10/2008
   exposure: 7730 s

2. obscode: 00038080002
   observation date: 11/02/2010
   exposure: 8447 s

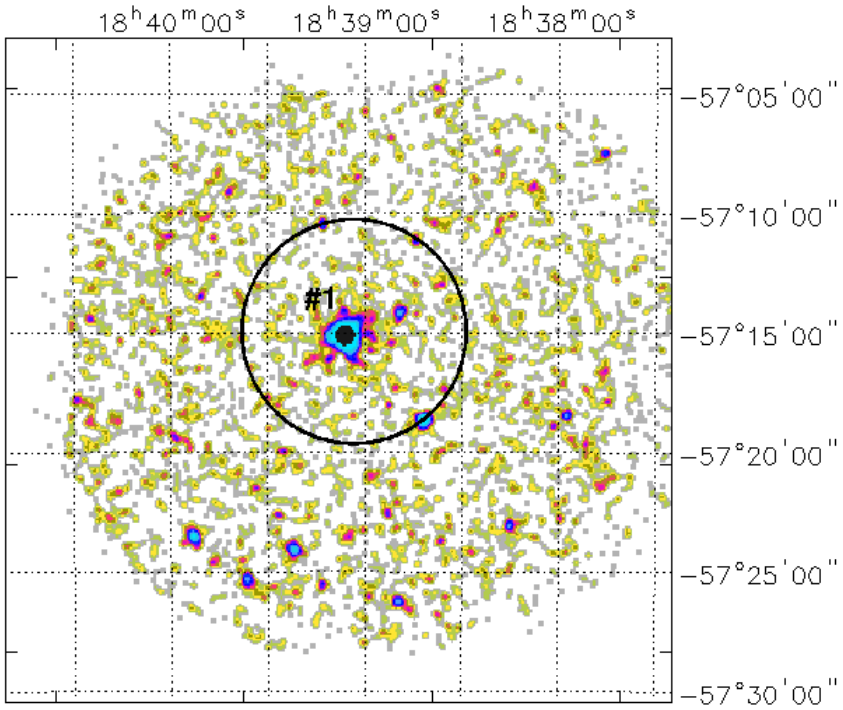

Figure 21: 0.3–10 keV XRT image of the SWIFT J1839.1+5717 field.

XRT detects a bright X–ray source, whose position falls within the 90% IBIS positional uncertainty, located at:

R.A.(J2000) = $18^h39^m06'.19$

Dec.(J2000) = $-57°15'05''.86$

error box = $3''.57$

It is detected at 34σ and 26.2σ c.l. in 0.3–10 keV energy band and above 3 keV, respectively.

Multi–wavelength counterparts to this XRT detection:

- USNO–A2.0 U0300.34665154 with magnitudes $R = 18.2$, and $B = 19.9$;
- WISE J183905.95–571505.0 with colours $W1 = 13.052 \pm 0.025$, $W2 = 11.210 \pm 0.021$, $W3 = 7.751 \pm 0.017$, and $W4 = 5.869 \pm 0.043$;
- 1SXPS J183905.8–571504.

The XRT spectrum is well modelled with an absorbed power law ($N_{\rm H(Gal)} = 7.26 \times 10^{20}$ cm^{-2}; $N_{\rm H(int)} = \left(2.06^{+0.36}_{-0.33}\right) \times 10^{22}$ cm^{-2}) having photon index $\Gamma = (1.57 \pm 0.22)$ and 2–10 keV flux of $\sim 8.4 \times 10^{-12}$ erg cm^{-2} s^{-1}.

IGR J20310+3835 (also PBC J2030.8+3834)

(IBIS detection: persistent)

Seven XRT observations available:

1. obscode: 00049381001
   observation date: 04/12/2012
   exposure: 126 s
2. obscode: 00049381002
   observation date: 05/12/2012
   exposure: 1043 s
3. obscode: 00049381003
   observation date: 06/12/2012
   exposure: 1570 s
4. obscode: 00049381004
   observation date: 07/12/2012
   exposure: 303 s
5. obscode: 00049381005
   observation date: 10/12/2012
   exposure: 692 s
6. obscode: 00049381006
   observation date: 11/12/2012
   exposure: 156 s
7. obscode: 00049381007
   observation date: 12/12/2012
   exposure: 1063 s

There are three X–ray detections compatible with either the 90% or the 99% IBIS positional uncertainties:

➢ Source #1, which lies within the 90% IBIS error circle, is located at:

R.A.(J2000) = $20^{\rm h}30^{\rm m}55'.27$

Dec.(J2000) = $+38^\circ33'44''.14$

error box = $4''.35$

It is detected at 8.2σ c.l. in 0.3–10 keV energy band, and it is still observed above 3 keV at 7.2σ c.l.

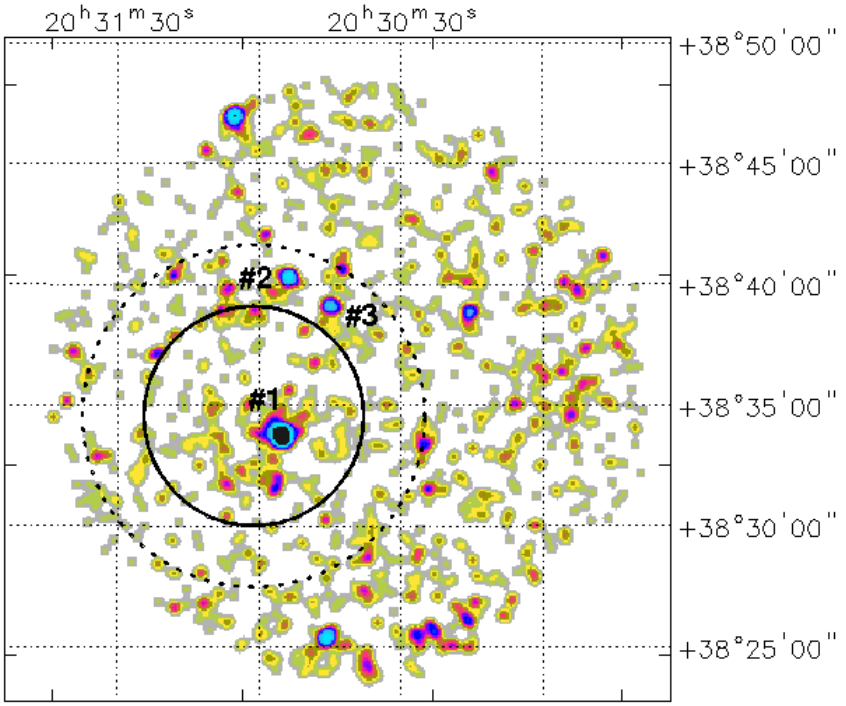

Figure 22: 0.3–10 keV XRT image of the IGR J20310+3835 field.

Multi–wavelength counterparts to this XRT detection:

- UGPS J203055.29+383347.1 ($J = 18.826 \pm 0.050$, $H = 17.297 \pm 0.022$, and $K = 16.544 \pm 0.040$), and UGPS J203055.30+383347.2 ($J = 18.710 \pm 0.048$, $H = 17.347 \pm 0.024$, and $K = 16.463 \pm 0.040$).

By fitting the XRT data with a power law passing only through Galactic absorption ($N_{\rm H(Gal)} = 1.04 \times 10^{22}$ cm^{-2}), we find a flat photon index ($\Gamma \sim 0.1$) and a 2–10 keV flux of $\sim 3 \times 10^{-12}$ erg cm^{-2} s^{-1}. If we freeze the photon index to 1.8, the data require an intrinsic column density $N_{\rm H(intr)} = \left(5.01^{+3.51}_{-2.58}\right) \times 10^{22}$ cm^{-2}; the 2–10 keV flux turns out to be around 2×10^{-12} erg cm^{-2} s^{-1}.

➢ Source #2, which is detected within the 99% IBIS error circle, is located at:

R.A.(J2000) = $20^{\rm h}30^{\rm m}44'.50$

Dec.(J2000) = $+38^{\circ}39'07''.80$

error box = $6''.00$

It is detected at 3.2σ in the 0.3–10 keV energy band; no detection is observed above 3 keV.

Multi–wavelength counterparts to this XRT detection:

- USNO–B1.0 1286–0413078 with magnitudes $R1 = 18.25$, $R2 = 18.08$, and $B2 = 20.59$;
- 2MASS J20304480+3839126 with magnitudes $J = 16.285 \pm 0.094$, $H = 15.766 \pm 0.135$, and $K = 14.726 \pm 0.000$;
- WISE J203045.13+383906.9 with colours $W1 = 11.040 \pm 0.024$, $W2 = 10.909 \pm 0.022$, $W3 = 10.834 \pm 0.453$, and $W4 = 7.271 \pm 0.000$;
- IPHAS2 J203044.82+383912.5 ($I = 17.84 \pm 0.02$), and IPHAS2 J203045.11+383906.9 ($I = 13.58 \pm 0.00$).

➢ Source #3, which is detected within the 99% IBIS error circle, is located at:

R.A.(J2000) = $20^{\rm h}30^{\rm m}53'.60$

Dec.(J2000) = $+38^{\circ}40'18''.70$

error box = $6''.00$

It is detected at 3.5σ c.l. in 0.3–10 keV energy band, and it is not observed above 3 keV.

Multi–wavelength counterparts to this XRT detection:

- USNO–B1.0 1286–0413123 with magnitudes $R2 = 19.32$, $B1 = 20.51$, and $B2 = 19.96$;
- IPHAS2 J203053.74+384020.3 ($I = 19.25 \pm 0.07$), IPHAS2 J203053.30+384019.6 ($I = 19.54 \pm 0.10$), and IPHAS2 J203053.06+384016.0 ($I = 20.05 \pm 0.15$);
- *ROSAT* Faint source 1RXS J203053.5+384032.

Apart from its behaviour in X–rays, no information has been collected from various databases about the nature of source #1 which we propose to be the most likely counterpart to IGR J20310+3835.

SWIFT J2233.9+1007

(IBIS detection: persistent)

Two XRT observations available:

1. obscode: 00041790001
   observation date: 12/01/2011
   exposure: 1029 s

2. obscode: 00041790002
   observation date: 24/01/2011
   exposure: 9646 s

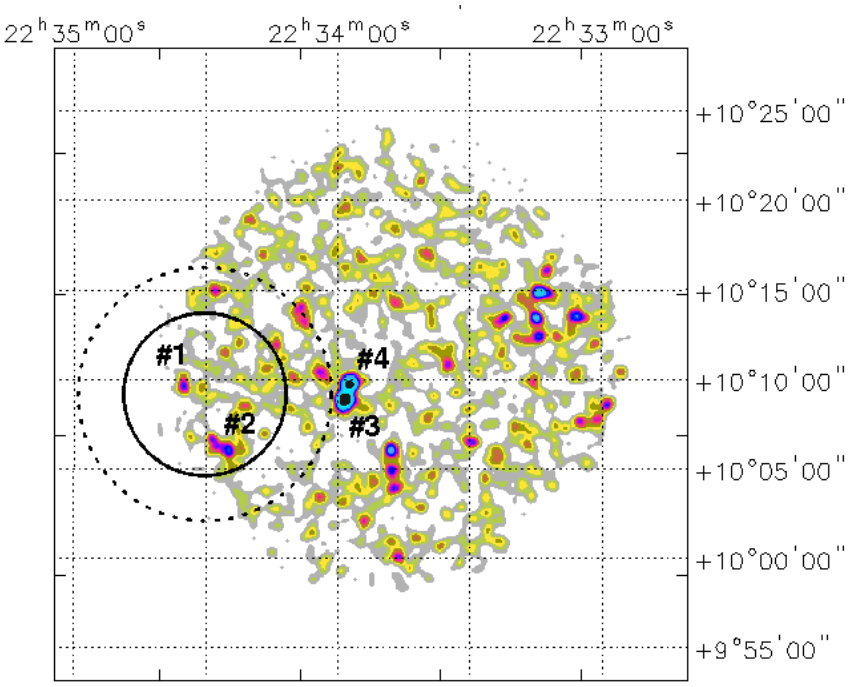

Figure 23: 0.3–10 keV XRT image of the SWIFT J2233.9+1007 field.

We note that, although the XRT observations are pointing at SWIFT J2233.9+1007, this source does not appear in any published *Swift*/BAT catalogues. We suggest changing the source name using the *INTEGRAL*/IBIS nomenclature.

XRT detects four X–ray sources whose positions are compatible with either the 90% or the 99% IBIS positional uncertainties:

➢ Source #1 is located within the 90% IBIS error circle at:

R.A.(J2000) = $22^h34^m34'.80$

Dec.(J2000) = $+10^{\circ}09'38''.80$

error box = $6''.00$

It is detected at 2.6σ c.l. in the 0.3–10 keV energy range, and it is not observed above 3 keV.

Multi–wavelength counterparts to this XRT detection:

- USNO–B1.0 1001–0613869 with magnitudes $R2 = 20.21$, $B1 = 20.36$, and $B2 = 20.05$;
- WISE J223434.88+100935.2 with colours $W1 = 15.907 \pm 0.055$, $W2 = 14.961 \pm 0.122$, $W3 = 11.898 \pm 0.320$, and $W4 = 8.561 \pm 0.000$;
- GALEXASC J223434.88+100936.3;
- 1SXPS J223434.9+100933.

From the X–ray data we can only infer a 2–10 keV flux of $\sim 4 \times 10^{-14}$ erg cm^{-2} s^{-1}, by assuming a power law ($N_{\rm H(Gal)} = 6.59 \times 10^{20}$ cm^{-2}) having the photon index frozen to 1.8.

➢ Source #2 is located within the 90% IBIS error circle at:

R.A.(J2000) = $22^{\rm h}34^{\rm m}24'.90$

Dec.(J2000) = $+10^{\circ}06'05''.40$

error box = $6''.00$

It is detected at 2.8σ c.l. in the 0.3–10 keV energy range, and it is not observed above 3 keV.

Multi–wavelength counterparts to this XRT detection:

- USNO–B1.0 1001–0613832 with magnitudes $R2 = 17.57$, and $B2 = 20.61$;
- WISE J223424.76+100600.2 with colours $W1 = 16.223 \pm 0.069$, $W2 = 15.591 \pm 0.192$, $W3 = 12.412 \pm 0.458$, and $W4 = 8.884 \pm 0.000$;
- 1SXPS J223425.0+100601.

Also in this case, from the X–ray data we can only infer a 2–10 keV flux of $\sim 2 \times 10^{-14}$ erg cm^{-2} s^{-1}, by assuming a power law ($N_{\rm H(Gal)} = 6.66 \times 10^{20}$ cm^{-2}) having the photon index frozen to 1.8.

➢ Source #3 is located just outside the 99% IBIS error circle at:

R.A.(J2000) = $22^{\rm h}33^{\rm m}57'.29$

Dec.(J2000) = $+10^{\circ}09'46''.13$

error box = $4''.31$

It is detected at 6.1σ c.l. in the 0.3–10 keV energy range, but it is not observed above 3 keV.

Multi–wavelength counterparts to this XRT detection:

- USNO–A2.0 U0975.20989483 with magnitudes $R = 17.3$, and $B = 17.3$;
- WISE J223357.50+100943.7 with colours $W1 = 14.255 \pm 0.029$, $W2 = 12.814 \pm 0.034$, $W3 = 9.846 \pm 0.056$, and $W4 = 7.362 \pm 0.119$;
- GALEXASC J223357.51+100944.1;
- 1SXPS J223357.3+100945.

➢ Source #4 is located at:

R.A.(J2000) = $22^{\rm h}33^{\rm m}58'.45$

Dec.(J2000) = $+10^{\circ}08'52''.90$

error box = $4''.26$

It is detected at 6.9σ and 3.1σ c.l. in the 0.3–10 keV energy band and above 3 keV. respectively.

Multi–wavelength counterparts to this XRT detection:

- USNO–A2.0 U0975.20989579 with magnitudes $R = 18.0$, and $B = 17.6$;
- WISE J223358.45+100852.1 with colours $W1 = 15.112 \pm 0.041$, $W2 = 13.715 \pm 0.054$, $W3 = 10.335 \pm 0.079$, and $W4 = 8.432 \pm 0.329$;
- GALEXASC J223358.36+100854.2 (QSO, $z = 1.854$);
- NVSS J223358+100852 (F(1.4 GHz) = 360.1 ± 10.8 mJy);
- CRATES J223358+100855 (F(4.8 GHz) = 360.1 mJy) Flat Spectrum Radio Source ($\alpha = -0.172$);
- 1SXPS J223358.4+100853.

Given their location within the 90% IBIS error circle, source #1 and #2 cannot be discarded as possible counterparts to SWIFT J2233.9+1007, although their faintness in X–rays, combined with the information gathered from the literature, does not give any insight into their nature. Source #4 seems a better chance, although it is outside the 99% IBIS error circle, but inside the likely BAT positional uncertainty.

1SWXRT J230642.8+550817

(IBIS detection: persistent)

Two XRT observations available:

1. obscode: 00039882001
   observation date: 01/09/2010
   exposure: 603 s

2. obscode: 00039882002
   observation date: 26/10/2010
   exposure: 353 s

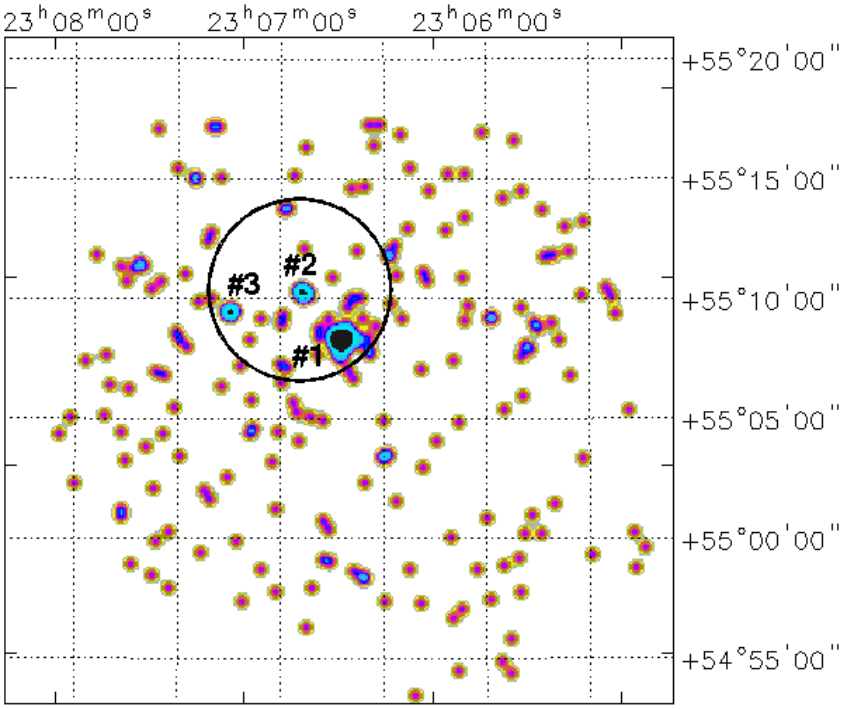

Figure 24: 0.3–10 keV XRT image of the 1SWXRT J230642.8+550817 field.

XRT detects three X–ray objects located within the 90% IBIS positional uncertainty:

➢ Source #1 is located at:

R.A.(J2000) = $23^h06^m42'.33$

Dec.(J2000) = $+55°08'18''.91$

error box = $4''.51$

It is detected at 8.4σ c.l. in 0.3–10 keV energy band, and it is still visible above 3 keV at 5.2σ c.l.

Multi–wavelength counterparts to this XRT detection:

- USNO–A2.0 U1425.14606199 with magnitudes $R = 16.6$, and $B = 17.3$;
- 2MASS J23064269+5508200 with magnitudes $J = 15.857 \pm 0.071$, $H = 15.688 \pm 0.161$, and $K = 15.392 \pm 0.181$;
- WISE J230642.67+550820.1 with colours $W1 = 15.145 \pm 0.042$, $W2 = 15.415 \pm 0.106$, $W3 = 11.537 \pm 0.105$, and $W4 = 9.442 \pm 0.405$;
- IPHAS2 J230642.70+550820.2 with magnitude $I = 16.47 \pm 0.01$;
- 1SXPS J230642.6+550818;
- This source is reported as an H_α emission line objects from IPHAS (Witham et al. 2008).

The XRT spectrum is well modelled with a power law passing through the Galactic absorption ($N_{\rm H(Gal)} = 3.11 \times 10^{21}$ cm^{-2}) having a flat photon index ($\Gamma = 1.10 \pm 0.43$) and a 2–10 keV flux of $\sim 6 \times 10^{-12}$ erg cm^{-2} s^{-1}.

➢ Source #2 is located at:

R.A.(J2000) = $23^{\rm h}06^{\rm m}53'.40$

Dec.(J2000) = $+55^\circ 10' 14''.80$

error box = $6''.00$

It is detected at 2.6σ c.l. in 0.3–10 keV energy band, and is not revealed above 3 keV.

Multi–wavelength counterparts to this XRT detection:

- USNO–A2.0 U1425.14610862 with magnitudes $R = 12.6$, and $B = 14.3$;
- 2MASS J23065374+5510178 with magnitudes $J = 10.170 \pm 0.018$, $H = 9.492 \pm 0.015$, and $K = 9.313 \pm 0.022$;
- WISE J230653.74+551017.9 with colours $W1 = 9.146 \pm 0.022$, $W2 = 9.153 \pm 0.021$, $W3 = 9.019 \pm 0.021$, and $W4 = 8.776 \pm 0.239$;
- IPHAS2 J230653.74+551012.3 ($I = 18.89 \pm 0.05$), and IPHAS2 J230653.71+551009.1 ($I = 19.26 \pm 0.07$);
- 1SXPS J230653.6+551015.

➢ Source #3 is located at:

R.A.(J2000) = $23^{h}07^{m}14'.60$

Dec.(J2000) = $+55^{\circ}09'27''.10$

error box = $6''.00$

This source is detected at 2.6σ c.l. in 0.3–10 keV; no detection is found above 3 keV.

Multi–wavelength counterparts to this XRT detection:

- USNO–A2.0 U1425.14619626 with magnitudes $R = 14.2$, and $B = 16.1$;
- 2MASS J23071478+5509277 with magnitudes $J = 12.182 \pm 0.022$, $H = 11.552 \pm 0.021$, and $K = 11.411 \pm 0.23$;
- WISE J230714.81+550927.7 with colours $W1 = 11.369 \pm 0.023$, $W2 = 11.392 \pm 0.022$, $W3 = 11.437 \pm 0.109$, and $W4 = 9.646 \pm 0.000$;
- 1PHAS2 J230714.81+550927.7 with magnitude $I = 13.29 \pm 0.00$;
- 1SXPS J230714.8+550926.

Source #1 is the only XRT detection still observed above 3 keV, which makes this objects the likely counterpart to 1SWXRT J230642.8+550817.

Bibliography

[1] Acero F., Ackermann M., Ajello M., et al. 2015, ApJS submitted, arXiv:1501.02003

[2] Barentsen G., Farnhill H. J., Drew J. E., et al. 2014, MNRAS, 444, 3230

[3] Baumgartner W. H., Tueller J., Markwardt C. B., et al. 2013, ApJS, 207, 19

[4] Bianchi L., Herald J., Efremova B., et al. 2011, Ap&SS, 335, 161

[5] Condon J. J., Cotton W. D., Greisen E. W., et al. 1998, AJ, 115, 1693

[6] Evans P. A., Osborne J. P., Beardmore A. P., et al. 2014, ApJS, 210, 8

[7] Healey S. E., Romani R. W., Taylor G. B., et al. 2007, ApJS, 171, 61

[8] Jones D. H., Read M. A., Saunders W., et al., 2009, MNRAS, 399, 683

[9] Jones D. H., Saunders W., Colless M., et al., 2004, MNRAS, 355, 747

[10] Kalberla P. M. W., Burton W. B., Hartmann D., et al. 2005, A&A, 440, 775

[11] Kozlowski S., Onken C. A., Kochanek C. S., et al. 2013, ApJ, 775, 92

[12] Lee K. J., Guillemot L., Yue Y. L., et al. 2012, MNRAS, 424, 2832

[13] Lucas P. W., Hoare M. G., Longmore A., et al. 2008, MNRAS, 391, 136

[14] Monet D. G., Levine S. E., Canzian B., et al. 2003, AJ, 125, 984

[15] Puccetti S., Capalbi M., Giommi P., et al. 2011, A&A, 528, A122

[16] Saxton R. D., Read A. M., Esquej P., et al. 2008, A&A, 480, 611

[17] Skrutskie M. F., Cutri R. M., Stiening R., et al. 2006, AJ, 131, 1163

[18] Verrecchia F., in't Zand J. J. M., Giommi P., et al. 2007, A&A, 472, 705

[19] Voges W., Aschenbach B., Boller Th., et al. 1999, A&A, 349, 389

[20] Watson et al. 2013, in prep

[21] Witham A. R., Knigge C., Drew J. E., et al. 2008, MNRAS, 384, 1277

[22] Wright E. L., Eisenhardt P. R. M., Mainzer A. K., et al. 2010, AJ, 140, 1868